A SYSTEMATIC METHOD FOR THE ANALYSIS OF HIGH-RESOLUTION FRAUNHOFER LINE PROFILES

C. DE JAGER
University Observatory 'Sonnenborgh', Utrecht, The Netherlands
and
L. NEVEN
Royal Belgian Observatory, Uccle-Brussels, Belgium

(Received 31 May, 1966)

Abstract. A fraunhofer line profile depends on various parameters, partly related to the photospheric structure (T, P_g, P_e, v_{conv}, v_{turb}), partly to the atom or ion involved (such as oscillator strength, energy levels), partly also resulting from the interaction of the relevant kind of particles with the photosphere, and the photospheric radiation field. In this paper we shall mainly pay attention to the determination of:

the macroturbulent (convective) velocities, $v_{conv}(\tau)$;
the damping constant $\gamma(\tau)$;
the abundance, A_{el};
the distribution function $\varphi(v_{conv},\tau)$ of the convective velocities at each depth τ;
the source function, $S(\tau)$;
the microturbulent velocities, $v_{turb}(\tau)$.

The particular difficulty with these unknowns is that they are, as a rule, coupled in the resulting line profiles, that is: the shapes and intensities in these profiles are determined by the *combined* influence of these unknowns (together with the other above-given parameters).

In this paper we describe a method to determine these six unknowns empirically by *separating* them, in analysing accurate high-resolution observations of line profiles of a multiplet. The unknown functions and quantities are consecutively determined in the above given succession. For each determination another, appropriate part of the line profile is used. In some cases the influence of the mutual coupling of the various parameters cannot be completely eliminated, and an iterative method has to be used.

The method is summarized in Table II and section 2, and is further explained in sections 3 to 8. It is applied to an infrared C I multiplet. The main results are the following:

(a) the convective velocities are zero for $\tau_0 < 0.1$; deeper they increase steeply to a maximum value of more than 3 km/sec at $\tau_0 \approx 0.15$; for greater depths there seems to be a slow decrease.

(b) The elements having these velocities must be smaller or much smaller than 0.″5.

(c) The convective motions are isotropic.

(d) The (micro-)turbulent velocity component is as assumed in the Utrecht Reference Photosphere 1964.

(e) The log of the abundance of C with respect to H is: $0.635 - 4 \pm 0.02$.

(f) The damping constant derived from the observations of this multiplet agrees reasonably well with the results of theoretical predictions.

(g) Deviations from Local Thermal Equilibrium occur only at depths less than $\tau_0 = 0.1$.

1. Introduction

The precise shape of a line profile in solar or stellar spectra depends on at least six parameters, most of which are functions of depth. The parameters are:

the abundance A_{el} of the relevant element;
the source function $S(\tau)$;

Solar Physics **1** (1967); © *D. Reidel Publishing Company, Dordrecht-Holland*

the convective velocity component $v_c(\tau)$;
the distribution function $\varphi(v_{conv})$ of convective velocities at each optical depth;
the (micro-)turbulent velocity component $v_t(\tau)$;
the damping constant $\gamma(\tau)$.

Naturally, there are still other parameters or constants which are equally important in defining a line profile, such as the excitation and ionisation potentials, the oscillator strength of the transition, and the statistical weight of the levels involved; furthermore, other functions defining the structure of the photosphere, such as the temperature, the gas- and electron pressures must be known.

In most cases this latter group of constants and functions may be considered known, at least in the first approximation. Anyway, they can, in principle, be determined from laboratory measurements, or from investigations of the solar continuous spectrum.

The particular difficulty with the six unknowns listed above is that they can only be determined from studying line profiles.

In this paper we describe a systematic method for finding these six unknowns from the observed line profiles and their centre-to-limb variation. In this connection we should like to stress that it is not *essential* for our method to have centre-to-limb observations available, and that the method would also be applicable to stellar spectra, provided that the spectral resolution and the photometric accuracy are sufficiently high as to warrant that the observed line profiles are very reliable. Naturally, it is more difficult to obtain information about the depth dependence of the unknowns from *stellar* spectra, than is the case in the *solar* spectrum.

As a rule the six unknowns A_{el}, $S(\tau)$, $v_c(\tau)$, $\varphi(v_c)$, $v_t(\tau)$ and $\gamma(\tau)$ influence the whole observed line profile, this means that they are coupled in the equations which determine the emergent spectrum. Hence, one *could* try to determine their values by computing theoretical line profiles as functions of arbitrarily chosen values of the six parameters, and, by trial and error, determine their best values. This method would be very labourious and is in practice impossible. Therefore, it is preferable to try to separate the variables, and to find them by investigating those parts or those properties of the line profiles that are solely or nearly completely determined by that particular unknown parameter. After having found the six unknowns, a detailed computation of the line profile should be performed, as a final test, and the result of such

TABLE I

Spectroscopic data of the C I multiplet near 10700 Å; transition: $3s^3P^0 - 3p^3D$. The *gf*-values were taken from GOLDBERG, MÜLLER and ALLER (1960)

wavelength	E.P. (electron volts)		j	log gf
10691.24	7.46	8.61	2–3	+ 0.32
10683.09	7.45	8.61	1–2	+ 0.05
10685.36	7.45	8.60	0–1	− 0.28
10729.59	7.46	8.61	2–2	− 0.41
10707.36	7.45	8.60	1–1	− 0.41
10754.02	7.46	8.60	2–1	− 1.58

a final computation could still lead to an improvement of values for one or more of the parameters. Such a method has been developed in the course of the last few years by the present authors.

As a test-case we chose the 6 lines of the C I-multiplet $3s^3P^0 - 3p^3D$ near 10700 Å. The main properties of this multiplet are shown in Table I. The observations are described in DE JAGER and NEVEN (1967). Preliminary reports on this investigation have appeared elsewhere; we determined first approximation values of

$v_c(\tau)$ from line asymmetries
$v_t(\tau)$ from line-core widths
} (DE JAGER and NEVEN, 1964);

$S(\tau)$
A_C
} from central intensities (DE JAGER and NEVEN, 1966a);

A_C
$\gamma(\tau)$
} from the line wings (DE JAGER and NEVEN, 1966b).

After having performed these preliminary investigations we realized that the sequence of computations followed in the above mentioned papers is not the most logical one. For a really *systematic* method, that should, at least in principle, be applicable to any high-resolution line profile in solar or stellar spectra, the sequence of operations should be arranged differently. This has been done in the present paper.

We believe that the method described here satisfies the demand that the determination of each of the parameters is separated from the others. In determining those parameters that *are* coupled (e.g. the line wing profiles are determined by the product of A_{el} and γ) we first derive one of the parameters from such a part of the line profile where it is not coupled with the other parameters (e.g. in the above example we first derive A_C from the weak lines of the multiplet and then find γ from the line wings).

The change of the sequence of operations naturally forced us to repeat the earlier computations referred to above; consequently some of the earlier results have changed, but in most cases only slightly. These new results are given in this paper. Furthermore, we pay special attention to an estimation of the uncertainties in the derived quantities, and the work should be completed by an exact integration of some parts of the line profile, on the basis of these parameters. This final computation should then serve as a test to see whether the solution found is really capable of describing the complete line profile with all its details.

As a last remark we should add that, though this systematic method is applied to a certain group of spectral lines (an infrared C multiplet) and some new results are communicated, it is not chiefly for these results that this paper has been written, but rather for giving an exposition of our method. The results would have to be confirmed by similar studies of other fraunhofer lines. These investigations are now under way.

2. General Course of the Systematic Analysis

Before starting with a detailed discussion we give, in Table II, a reviewing summary of the method developed in this paper.

TABLE II

Review of consecutive steps in the analysis

unknown function or quantity	symbol	determined from	part of line	other parameters influencing result	remarks see text	section
convective (or: macro-turbulent) velocities	$v_c(\tau)$	line asymmetries	$0.7 \lesssim \frac{i}{i_0} \lesssim 0.95$	$\varphi(v_c)$	1	3
product of damping constant and abundance	$\gamma(\tau) \cdot A_C$	line wings	$\frac{i}{i_0} \lesssim 0.95$			4
abundance	A_C	core of weak line	$\lvert\Delta\lambda\rvert \lesssim 0.05$ Å	v_c, v_t, S	2	5,7
distribution function of convective velocities	$\varphi(v_c)$	shape of weak line	medium part			5
source function	$S(\tau)$	central intensities of strong lines	$\Delta\lambda = 0$	v_c, A, (v_t)	3,4	6,7
(micro-)turbulent velocities	$v_t(\tau)$	cores of strong lines	$\frac{i}{i_0} \lesssim 0.7$	S	4	8

To this Table we should add the following *remarks* (see the numbers in column 5 of Table II):

(1) The result on $v_c(\tau)$ will be influenced by the assumption about the distribution function $\varphi(v_c)$, e.g. a two-element model will need another $v_c(\tau)$ curve than a three-element model.

(2) The abundance will be determined by using the weakest line of the multiplet; this line, at 10754.02 Å is so weak that the source function $S(\tau)$ is equal to the Planck function $B(\tau)$ in the region where the line is formed (this is shown in section 6); furthermore, the turbulent velocity v_t is small in this region. If the line is situated on the linear part of the curve of growth knowledge of v_t is not even necessary for determining A_c. Hence an acceptable assumption on $v_t(\tau)$ will be sufficient for a reliable determination of A_C.

(3) The source function is determined from the central intensities of strong lines. The absorption in the line centre is also determined by the turbulent velocities but not strongly so. Hence a reasonable assumption about $v_t(\tau)$ will be sufficient for a first approximation of $S(\tau)$.

(4) The turbulent velocities should only be determined with the Goldberg-Unno method in that region of the line profile where the method *can* be applied, that is, where the line asymmetry, due to convective velocities is zero. The allocation of optical depths to the v_t-values found depends on the assumed $S(\tau)$ relation. Hence $v_t(\tau)$ depends greatly on $S(\tau)$.

Once $v_t(\tau)$ being found a new determination of $S(\tau)$ should be made. This iteration should converge very rapidly, since S depends only weakly on $v_t(\tau)$. In the present paper even this iteration did not appear necessary: the $v_t(\tau)$ curve found in first order approximation turns out to be virtually equal to the adopted zero-order $v_t(\tau)$ curve.

Testing of the results: A final test of the results should include the complete theoretical computation of the line profiles on the basis of the values found for the six parameters. This part of the investigation is not shown in this paper.

3. The Convective or Macroturbulent Velocities v_c

By *convective velocities* we mean the part of the velocity field that produces a sight-line motion of the whole relevant part of the photosphere from which the lines originate. Such motions could as well be called *macroturbulent* velocities. By calling them in either way we do not want to prejudice upon the interpretation of the observed phenomena.

The convective velocities were derived from the asymmetries of the spectral lines. All investigated lines show a small but distinct asymmetry, which is moreover a function of depth in the line profile. This asymmetry is a real property of the line since it does not disappear after the profile has been corrected for the influence of the apparatus profile. It is shown clearly by Figure 1, that the deep part of the corrected profile (for $r = i/i_0 < 0.75$) is no longer asymmetric (crosses in Figure 1) but

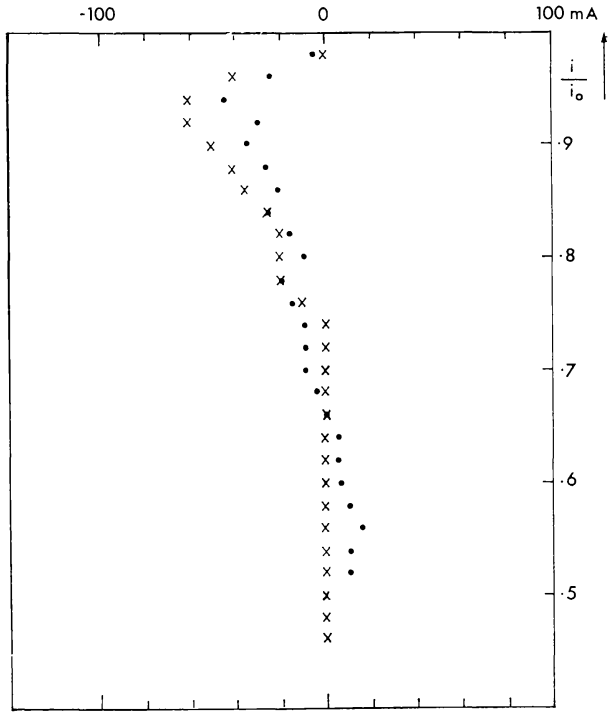

Fig. 1. As an example this figure shows the measured asymmetry in the profile of the C line at λ 10691 at cos $\theta = 1.00$. Dots give the asymmetry found before the correction for the apparatus profile; crosses give the asymmetry of the corrected profile. Abscissa: wavelength distance in mA.

that the asymmetry is noticable in the upper part. This proves (1) that the apparatus-profile corrections are needed, and (2) that the asymmetry of the corrected profiles is a real phenomenon. The asymmetry reflects the convective or large-scale motions in the photosphere. These are expected to be zero in the high atmosphere (hence: for large values of $(1-r)$), and larger deep in the atmosphere. However, the convective velocities cannot be derived directly from the asymmetry, since their derivation presupposes knowledge of the contribution of the hot and cold elements of the photosphere to the observed line.

For each line, for each value of cos θ and for a series of depressions $d\,(=1-r)=$ 0.10, 0.15, ... etc., the line asymmetry $\Delta\lambda$ was measured. Here $\Delta\lambda$ is defined as the wavelength distance from the axis of the line to the unshifted position of the line centre. Hence $\Delta\lambda=\frac{1}{2}(\lambda_{\text{red}}(i)+\lambda_{\text{violet}}(i))$. We were not able to measure absolute values of the line displacements, but we assumed that $\Delta\lambda=0$ for the deep parts of the line profile, which assumption seems to be reasonable (see Figure 1).

These asymmetries, then, were converted into quantities, v' having the dimension of a velocity, and defined as

$$v' = c\,\frac{\Delta\lambda}{\lambda}.$$

These v' values are not the real convective velocities v_c, but are related to them in a way still to be defined. In order to find v_c we have to determine the relation between v' and the average optical depth τ_0^* to which this quantity refers. As a matter of fact v' is the result of an integration over the depth of the whole photosphere, but a sufficient approximation for τ_0^* is obtained if we assume that the intensity $I\,(\Delta\lambda)$ in the line profile, at the wavelength distance $\Delta\lambda$ from the line centre is equal to the source function S at the average optical depth of formation τ_0^*. Furthermore we shall assume L.T.E., hence $S=B$, at least in the layers where the line asymmetry originates. This assumption finds its justification in section 6 of this paper, where it will be shown that deviations from L.T.E. are only of importance for $\tau_0 \lesssim 0.1$.

Furthermore we shall show in this section that convection is unimportant in this uppermost part of the photosphere.

The residual line intensity $r = i/i_0$ has to be multiplied by i_0, the continuous intensity at 10 700 Å, to give the emergent intensity. For i_0 we took the continuum intensity computed for the Utrecht Reference Photospheric model 1964 (U.R.P. 1964: HEINTZE, HUBENET and DE JAGER, 1964). In our previous analysis of the macro-turbulent velocities (DE JAGER and NEVEN, 1964) we took for i_0 the *measured* continuum intensity, which seems better from the formal point of view, but since the measured continuum intensity at 10 700 Å and those computed for the U.R.P. model deviate still by a few percent, using the observed continuum would give rise to systematic errors in the result, because all other computations have been based on the U.R.P. model. In a way this shows the tentative character of detailed photospheric analyses based on Fraunhofer line studies.

Figure 2 gives v' as a function of the average optical depth of formation τ_0^*. The

τ_0^* scale differs from that previously given because of the reasons just given. There is a considerable scatter of the data but this is not surprising since the measured asymmetries are very small ($v'=0.38$ km/sec corresponds to an asymmetry of 0.01 Å). The relatively good agreement between results found for different cos θ-values looks fairly satisfactory.

The average trend is that $v'\approx 0$ for $\tau_0 \lesssim 0.1$, and increases further with depth. The mean $v'(\tau_0^*)$ values, derived from averaging observations made at different cos θ but corresponding to the same τ_0^* values are given in Table III.

TABLE III

Depth dependence of the observed asymmetries of the *C*-lines, and deduced macrotubulent velocities for two different distribution functions of the velocities: $A_1 = 0.5$ corresponds to a two-element model; $A_1 = 0.33$ to a three-element model

τ_0	$v' = \frac{\Delta\lambda(\tau_0)}{\lambda} \cdot c \left(\frac{\text{km}}{\text{sec}}\right)$	v_c (km/sec) for:	
		$A_1 = 0.33$	$A_1 = 0.5$
0.080	$+0.05 \pm 0.06$	—	—
0.125	-0.17 ± 0.1	$+3.5 \pm 2.0$	$+2.3 \pm 1.4$
0.17	-0.38 ± 0.1	$+4.1 \pm 1.1$	$+2.8 \pm 0.7$
0.26	-0.6 ± 0.2	$+3.8 \pm 1.3$	$+2.5 \pm 0.8$
0.43	-0.55 ± 0.2	$+1.7 \pm 0.6$	$+0.76 \pm 0.3$

One result that immediately catches the eye is that large-scale motions are apparently absent in photospheric layers above $\tau_0 = 0.1$. This upper boundary lies much higher than the upper boundary assumed in Mrs. Böhm-Vitense's theoretical model of the convection zone. Another result, also very important, is that there is *no* systematic difference between v'-values belonging to the same optical depths but derived from observations at different values of cos θ. This shows that the large-scale velocities are *not* simply directed up- and downward, but that they are *isotropic*, at least in the observable part of the photosphere ($\tau_0^* \lesssim 0.3$ to 0.5), which forms the very uppermost layer of the convection zone. This observation could be an argument for the interpretation of these velocities in terms of (macro-)turbulence rather than convection.

The next problem is to find the relation between the observed asymmetries and the real convective velocities. This problem has been tackled by us in the following way: Since all *C* is virtually neutral in the upper parts of the solar photosphere, the relative contribution to the line absorption coefficient of the various kinds of elements is proportional to the area A_i of the element considered, and to the factor $10^{-7.45\theta_i}$, where 7.45 is the excitation potential of the lower level of the transition considered, and $\theta_i = 5040/T_i$. With a three-column model, the resulting contribution to the convective velocity at any depth is approximately given by

$$v' = \frac{A_1 v_1\, 10^{-7.45\,\theta_1} - A_3 v_3\, 10^{-7.45\,\theta_3}}{\sum_{i=1}^{3} A_i\, 10^{-7.45\,\theta_i}}. \tag{1}$$

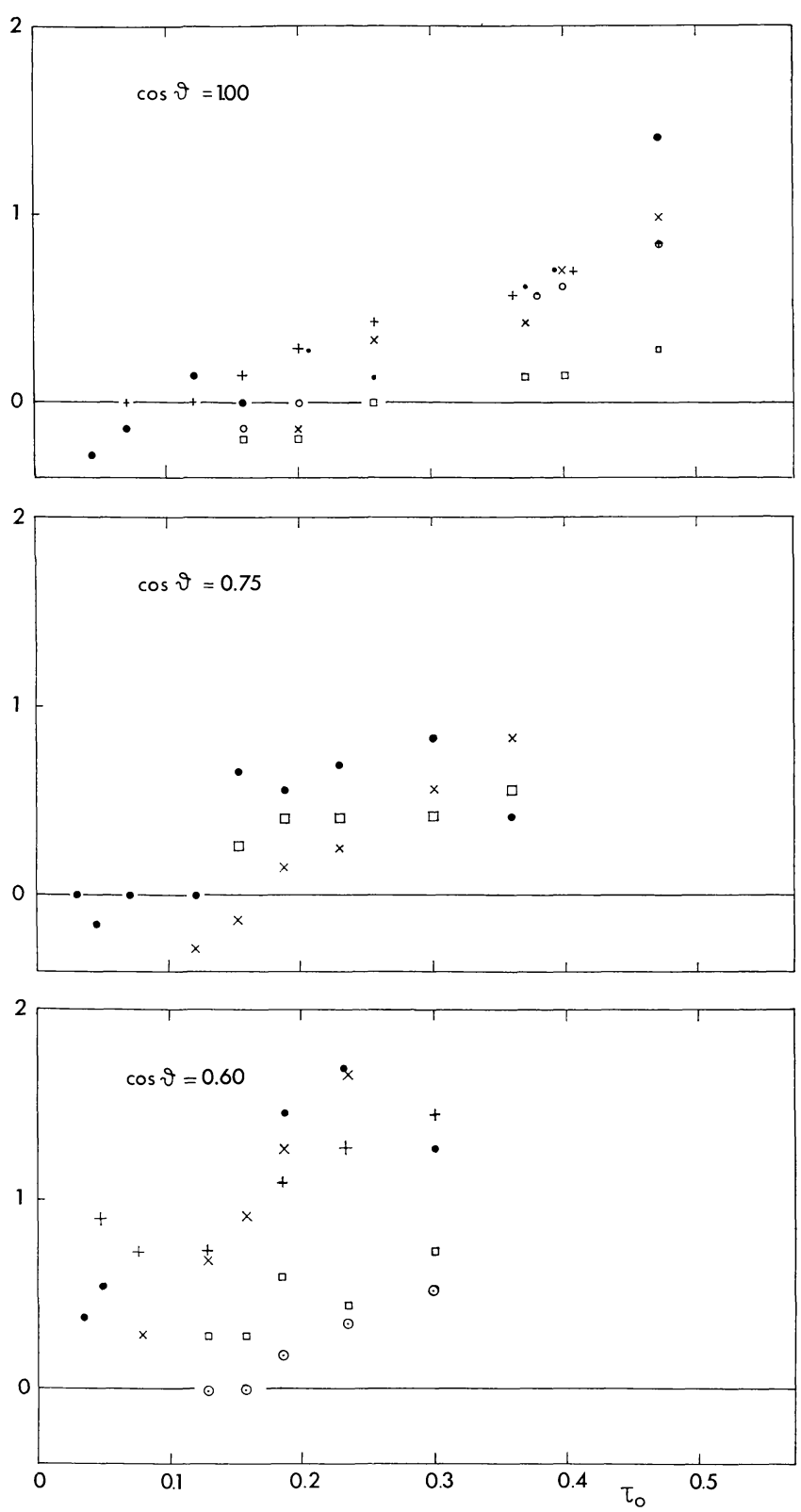

Fig. 2. Deduced values of v' (= asymmetry, expressed in km/sec), determined from the various lines and plotted against τ_0 for the U.R.P. Model. The main results are: (a) v' is about zero for $\tau_0 < 0.1$ and increases with increasing τ_0; (b) there is no clear anisotropy in the large scale motions: the average value of $v'(\tau_0)$ seems the same at each value of cos θ. The asymmetries are small: $v' = 1$ km/sec corresponds with an asymmetry of 0.03 Å.

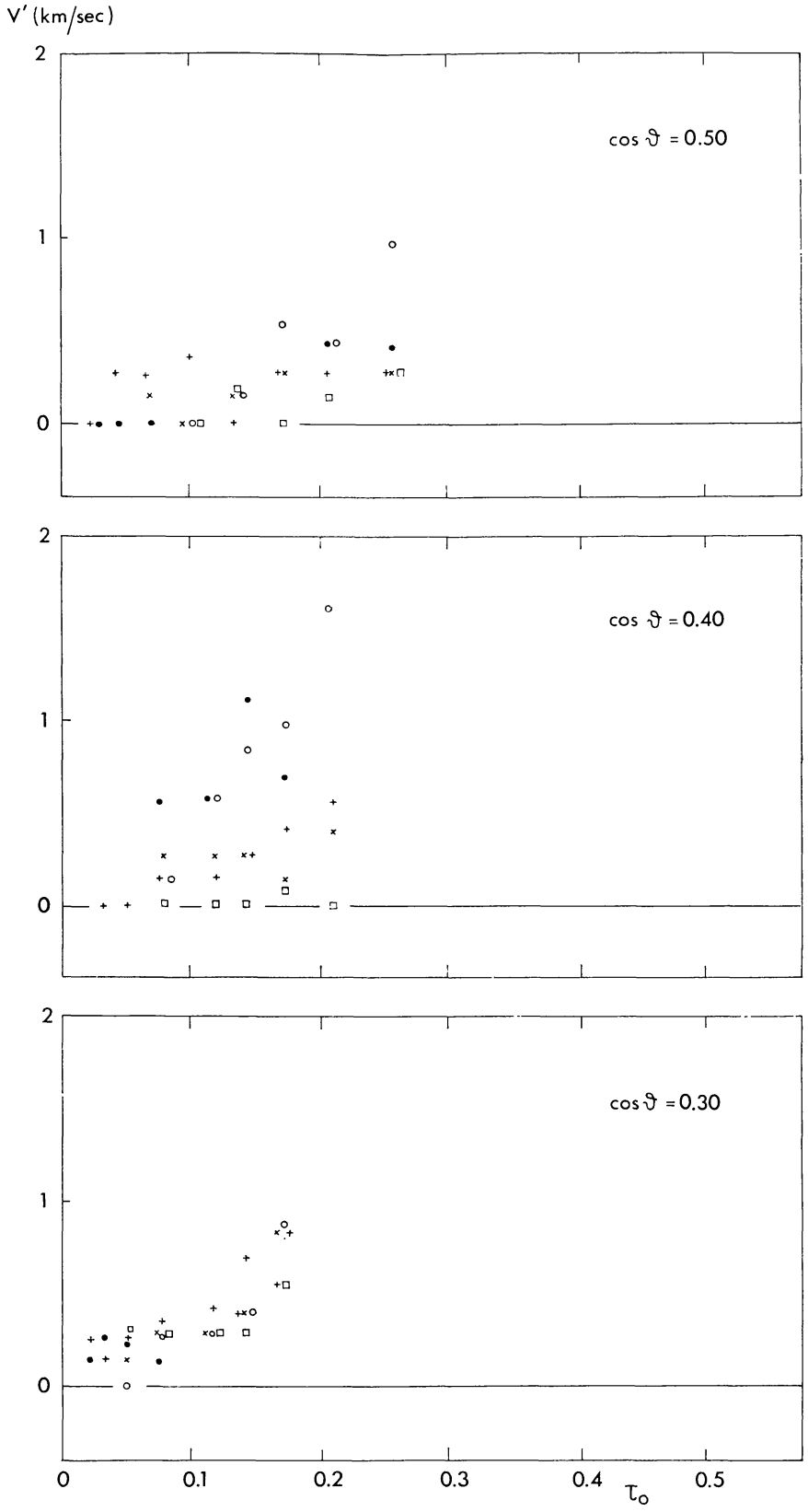

Fig. 2b

Here we have assumed that column 2 is not subjected to up- or downward motions. Obviously A_1, A_2 and A_3 are unknown, but we assume conservation of mass and hence

$$A_3 v_3 = A_1 v_1 \frac{\rho_1}{\rho_3}, \tag{2}$$

where $\rho = P_g \mu / RT$ is the density.

With Equation (2) the Equation (1) becomes

$$v' = \frac{A_1 v_1 (10^{-7.45\,\theta_1} - \frac{\rho_1}{\rho_3} 10^{-7.45\,\theta_3})}{\sum_{i=1}^{3} A_i\, 10^{-7.45\,\theta_i}}. \tag{3}$$

Equation (3) gives a relation between v_1, the convective velocity of one of the elements and the observed line asymmetry v'. To solve v_1 from the observed v' values we have to make an assumption, either about A_1 or about θ_1. We thought it to be the safest assumption to take θ_1 from the U.R.P. model since the temperature fluctuations in this model explain reasonably well the measured intensity fluctuations in the granulation, at least in the centre of the disc. We shall take A_1 as a parameter, and assume either $A_1 = 0.5$ (two-element model), or $A_1 = 0.33$ (three-element model).

The resulting v_1-values and their mean errors are shown in the last two columns of Table III and will also be shown in Figure 5, section 5. Although the values decrease with increasing depth above $\tau_0 = 0.1$, their mean errors are large so that a clear depth dependence cannot be considered as demonstrated. We provisionally assume the empirically determined convective velocity to be *constant with depth* (for $\tau_0 > 0.1$) and equal to the weighted mean value:

2.0 $\pm$ 0.3 km/sec (m.e.) for a two-element photospheric model, or
3.1 $\pm$ 0.4 km/sec (m.e.) for a three-element model.

In reality the solar photosphere will consist neither of two kinds of elements only, nor of three elements, since it is likely that we have more complicated distribution functions for temperatures and velocities. However, a determination of such functions would make extremely high demands both upon the quality of the observations as well as upon the theory used. An attempt to decide between the two possibilities, and to refine slightly the distribution function of the macroturbulent velocities will be made in section 5.

4. Determination of the Product $A_C \times \gamma(\tau_0)$

As a next step we discuss the extreme wings of the line profiles, and determine from these the product $A_C \cdot \gamma(\tau_0)$. The separation between A_C and $\gamma(\tau_0)$ can only be made after A_C has been found (see section 5).

4.1. THE ABSORPTION COEFFICIENT IN THE WINGS OF FRAUNHOFER LINES

In the well-known notation the absorption coefficient $\kappa(v)$ at a displacement $v = \Delta\lambda/\Delta\lambda_D$ in the region of a Fraunhofer line is given by

$$\kappa(v) = \kappa_c H(a, v), \tag{4}$$

where κ_c is the absorption coefficient in the line center.

For large values of v, and for $a \ll 1$:

$$H(a, v) = \frac{a}{\sqrt{\pi v^2}}. \tag{5}$$

Furthermore

$$a = \frac{\gamma}{2\Delta\omega_D} = \frac{\gamma\lambda^2}{4\pi c\Delta\lambda_D}, \tag{6}$$

$$v = \Delta\lambda/\Delta\lambda_D, \tag{7}$$

$$\kappa_c = \frac{\sqrt{\pi}e^2}{mc^2}\frac{\lambda^2\mathfrak{N}}{\Delta\lambda_D}(1 - e^{-c_2/\lambda T}),$$

$$= \frac{\sqrt{\pi}e^2\lambda^2}{mc^2\Delta\lambda_D} g f A_{el} \frac{b_{r,s}}{g}\frac{B}{4+B}\frac{1}{m_H}(1 - e^{-c_2/\lambda T}), \tag{8}$$

where $\mathfrak{N}$ is the number of classical oscillators per gram; A_{el} is the abundance of the element $= N_{el}/N_H$; $b_{r,s}$ is the fraction of the atoms in the relevant ionization and excitation level; $B = N_H/N_{He}$; m_H is the mass of the hydrogen atom. The other symbols have their usual meaning.

Combining Equations (4)–(8) one obtains

$$\kappa(\Delta\lambda) = C_1\lambda^4 \frac{\gamma g f A_{el}}{\Delta\lambda^2}\frac{b_{r,s}}{g}(1 - e^{-c_2/\lambda T}), \tag{9}$$

with

$$C_1 = \frac{e^2}{4\pi mc^3}\frac{B}{4+B}\frac{1}{m_H} = 0.26,$$

if we assume that B is 5.5 (Unsöld mixture). If we further introduce the "wing-parameter"

$$V = 0.26\frac{\gamma f g A_C}{\Delta\lambda^2}, \tag{10}$$

Equation (9) becomes:

$$\kappa(\Delta\lambda) = \lambda^4\frac{b_{r,s}}{g}(1 - e^{-c_2/\lambda T})V. \tag{11}$$

This formula is applicable to all spectral lines, provided that one confines oneself to that part of the line profile where the wing approximation $\kappa \sim \Delta\lambda^{-2}$ is correct.

4.2. THE EMPIRICAL DETERMINATION OF $\gamma(\tau_0)$

For an assumed value of V and for a given model of the photosphere, one can easily compute by numerical integration the corresponding selective optical depth:

$$\tau(V) = \int_0^{\tau_0} \frac{\kappa(V)}{\kappa_0} \, d\tau_0 ,$$

where κ_0 and τ_0 are the absorption coefficient and optical depth for $\lambda = 5000$ Å. Similarly one finds the continuous optical depth τ_λ for the continuous spectrum at 10700 Å. With $\kappa = \kappa_\lambda + \kappa(V)$, and $\tau = \tau_\lambda + \tau(V)$ one derives the relative line depression $d(V)$ with

$$d(V) = \frac{\int_0^\infty B(\tau_0) e^{-\tau_\lambda \sec\theta} \sec\theta \, d\tau_\lambda - \int_0^\infty B(\tau_0) e^{-\tau \sec\theta} \sec\theta \, d\tau}{\int_0^\infty B(\tau_0) e^{-\tau_\lambda \sec\theta} \sec\vartheta \, d\tau_\lambda} . \tag{12}$$

In Equation 12 we have introduced B instead of S and, hence, have assumed L.T.E. This is justified by our finding (see section 6) that $S \neq B$ only for $\tau_0 < 0.2$, and, as will be shown further on, that the depression d is formed mainly in very deep layers, where $\tau_0 > 0.6$ (see the average τ_0-values, denoted by τ_0^*, and given in the last two lines of Table II). It is important to have an impression of the average depth of formation τ_0^* of the line depression. This may be found in good approximation as follows:

If we call

$$\Delta(\tau_0) = B(\tau_0) \, e^{-\tau_\lambda(\tau_0) \sec\theta} - B(\tau_0) \, e^{-\tau(\tau_0) \sec\theta} ,$$

then

$$\tau_0^* = \frac{\int_0^\infty \tau_0 \Delta(\tau_0) \, d\tau_0}{\int_0^\infty \Delta(\tau_0) \, d\tau_0} . \tag{13}$$

The procedure of the investigation was as follows. First we computed the $d(V)$ and the $\tau_0^*(V)$ relation. The computations were made for the Utrecht Reference Model 1964 of the Photosphere (HEINTZE, HUBENET and DE JAGER, 1964) separately for each of the three columns of this model. We chose a small value of V and assumed a sec θ value. For these values the corresponding value of the depression d was computed with the IBM 1620 computer of the Uccle Observatory. If d was smaller than 10^{-3},

the computation was repeated for a new V-value, three times larger than the previous one; if d was greater than 10^{-3}, the resulting values of d and of τ_0^* were printed and the computations were repeated for a new value of V, which was 1.4 times larger than the previous value. This procedure was repeated until a value of d was reached exceeding 0.08, the arbitrarily chosen upper limit.

The computations were made for the three columns of the U.R.P. 1964 model, and for six values of cos θ, ranging from 0.3 to 1.0. In Figure 3 we show, as an example, the resulting values of d and of τ_0^* as a function of V for the three columns of the model

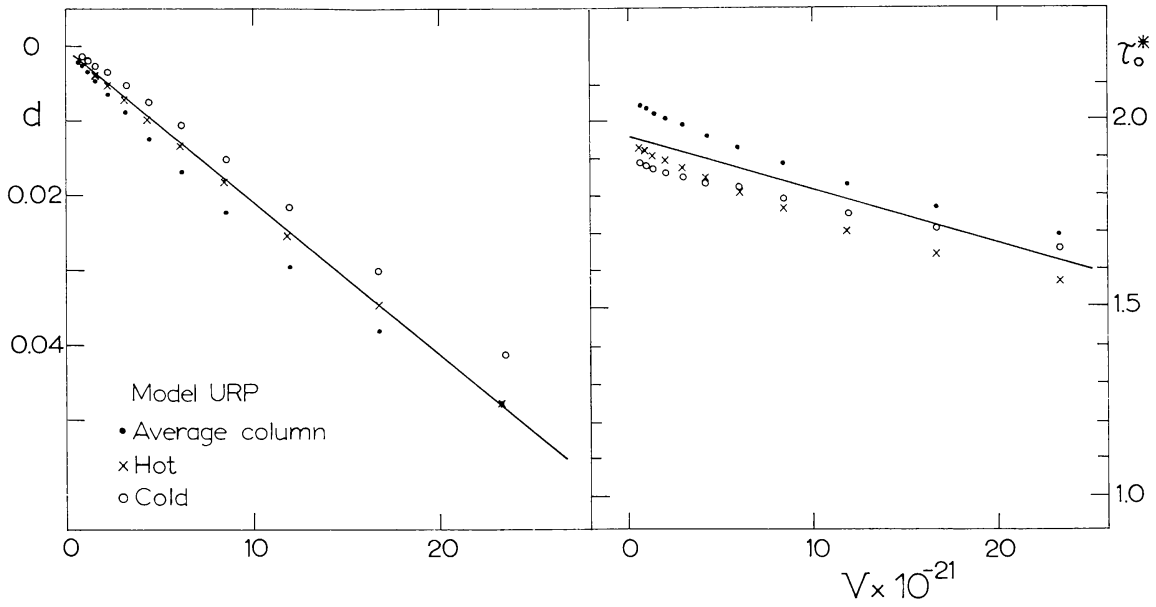

Fig. 3. Computed values of the line depression as a function of the wing parameter V for the three elements of the U.R.P. model; for cos $\theta = 1.00$.

in the case cos $\theta = 1.00$. The differences between the d (τ_0^*) values for the three columns are small but by no means negligible; at certain V-values the ratio between the extreme values amounts to a factor 2.

The relative contribution of the three kinds of photospheric columns is unknown but we assumed them to be equally important, i.e. we took a three-element model with $A_1 = 0.33$ and determined the straight mean value of the depressions (solid curve) which we call $\bar{d}$. We do not show the results for other values of cos θ; they appear to be nearly identical to those found for the disc centre, at least for $d < 0.05$. This is apparently due to the fact that the gradient of $B(\tau_\lambda)$ is nearly constant in the relevant parts of the photosphere.

For $\bar{d}$-values smaller than about 0.05 it appears possible to write $\bar{d} = K.V$, where K is a constant.

In order to determine γ the following procedure was followed. The observed depressions d in the extreme line wings were represented by:

$$d_{\text{obs}} = c.(\Delta\lambda)^{-2}$$

TABLE IV

c-values for the C I lines [Å^2]

λ	$\cos\theta = 1.0$	0.75	0.60	0.50	0.40	0.30
10691	0.0240	0.0215	0.0240	0.0150	0.0150	0.0110
10683	0.0235	0.0145	0.0095	0.0095	0.0110	0.0090
10685	0.0095	0.0067	0.0025	0.0030	0.0056	0.0058
10730	0.0078	0.0063	0.0062	0.0053	0.0045	0.0030
10707	0.0095	0.0075	0.0016	0.0066	0.0057	0.0025

We know further that

$$\tilde{d} = K.V \tag{15}$$

Here c and K are constants.

From the Equations (14) and (15) making $d_{obs} = \tilde{d}$ we derive:

$$V = c/K(\Delta\lambda)^2 . \tag{16}$$

Combining Equation (16) with Equation (10) one obtains

$$A_C\gamma = c/(0.26\, f\, g K) . \tag{17}$$

Here, all right-hand member quantities are known, so that A_C may be found: The c-values are given in Table IV, and the values of K, derived from the computations described in this paper are given in the second line of Table V.

TABLE V

Iterative determination of $A_C\gamma$, and τ_0*; the Table gives the mean values of $A_C\gamma$, derived from the five lines, observed at the same value of $\cos\theta$

$\cos\theta$	1.0	0.75	0.60	0.50	0.40	0.30
$K \times 10^{24}$	2.15	2.2	2.27	2.4	2.4	1.8
$(A_C\gamma)_1 \times 10^{-6}$	1.74	1.17	0.69	0.88	1.06	0.97
τ_0*	1.9	1.5	1.3	1.1	0.9	0.7
$K \times 10^{24}$	2.8	2.9	2.6	2.1	1.8	1.3
$(A_C\gamma)_2 \times 10^{-6}$	2.61	1.89	1.32	1.90	2.30	2.23
τ_0*	2.3	1.8	1.6	1.3	1.1	0.8
$K \times 10^{24}$	2.7	2.7	2.4	2.1	1.7	1.3
$(A_C\gamma)_3 \times 10^{-6}$	2.70	2.03	1.43	1.90	2.43	2.23
τ_0*	2.3	1.8	1.6	1.3	1.1	0.8

4.3. Iterative determination of $A_C\gamma(\tau)$

With the c- and K-values from Tables IV and V, and with the average optical depth of formation τ_0^* computed with Equation (13), one immediately derives from Equation (17) the values of $A_C\gamma(\tau_0^*)$. It then appears that $A_C\gamma$ is not a constant function of the optical depth, which is contrary to the assumption underlying the present derivation,

where a constant value of $A_C\gamma(\tau_0)$ was presupposed. Hence, for a correct determination of $A_C\gamma(\tau_0^*)$ we have to proceed by iteration.

We consider the derived values of $A_C\gamma(\tau_0^*)$ as first approximations. A smooth line, called $(A_C\gamma)_1(\tau_0)$, is drawn through the points; the value at $\tau_0 = 1$ (arbitrarily chosen) is called $(A_C\gamma)_1(1)$.

We next *define:*

$$\psi_1(\tau_0) = (A_C\gamma_1(\tau_0))/(A_C\gamma_1(1)).$$

Next, we repeat the procedure described in the preceding part of this section; however, in expression (11) and in all subsequent expressions $\kappa(\Delta\lambda)$ is replaced by $\kappa(\Delta\lambda)\cdot\psi_1(\tau_0)$.

We thus find from Equations (17) and (13) *new* values $A_C\gamma(\tau_0^*)$. These are not yet the second approximation: this is found by a multiplication of these values by $\psi_1(\tau_0)$, yielding:

$$(A_C\gamma)_2(\tau_0^*) = A_C\gamma(\tau_0^*)\cdot\psi_1(\tau_0).$$

Again we draw a smooth line through the points $(A_C\gamma)_2(\tau_0^*)$ and thus define a curve $(A_C\gamma)_2(\tau_0)$, a value $(A_C\gamma)_2(1)$, and a function $\psi_2(\tau_0)$.

The iteration is continued until for all τ_0^*:

$$|(A_C\gamma)_n(\tau_0^*)_n - (A_C\gamma)_{n-1}(\tau_0^*)_{n-1}| < \varepsilon,$$

where ε is a small quantity. Three approximations appear to be sufficient.

In practice we encounter the problem of how to extrapolate the function ψ outside the optical depth region defined by the τ_0^*-values. To that aim we assumed, on the basis of theoretical expectations, that for small τ_0-values

$$\gamma(:)P_g$$

and that for large τ_0-values

$$\gamma(:)P_e.$$

These assumptions are necessary but not critical.

The resulting $A_C\gamma(\tau_0^*)$ values found in three approximations are given in Table V; the last-approximation data are also shown in Figure 4, together with the extrapolation curve used.

One comment we should make in this graph is that it is surprising how deep the average optical depth of formation of the line wings is: the τ_0^* values go up to 2.3. This shows that it is indeed possible to investigate empirically the *deep* photospheric layers, by concentrating on the line *wings*.

Next we make a brief comparison of our derived $A_C\gamma(\tau_0)$ values with the results of theoretical predictions. Thereby we shall make use of our later finding (section 7), that $\log A_C = 0.635 - 4$.

Roughly, one may state that $\gamma(\tau)$ consists of two components, $\gamma_{H,He}(\tau)$, which is due to collisional damping by passing neutral particles, and $\gamma_e(\tau)$ which is due to

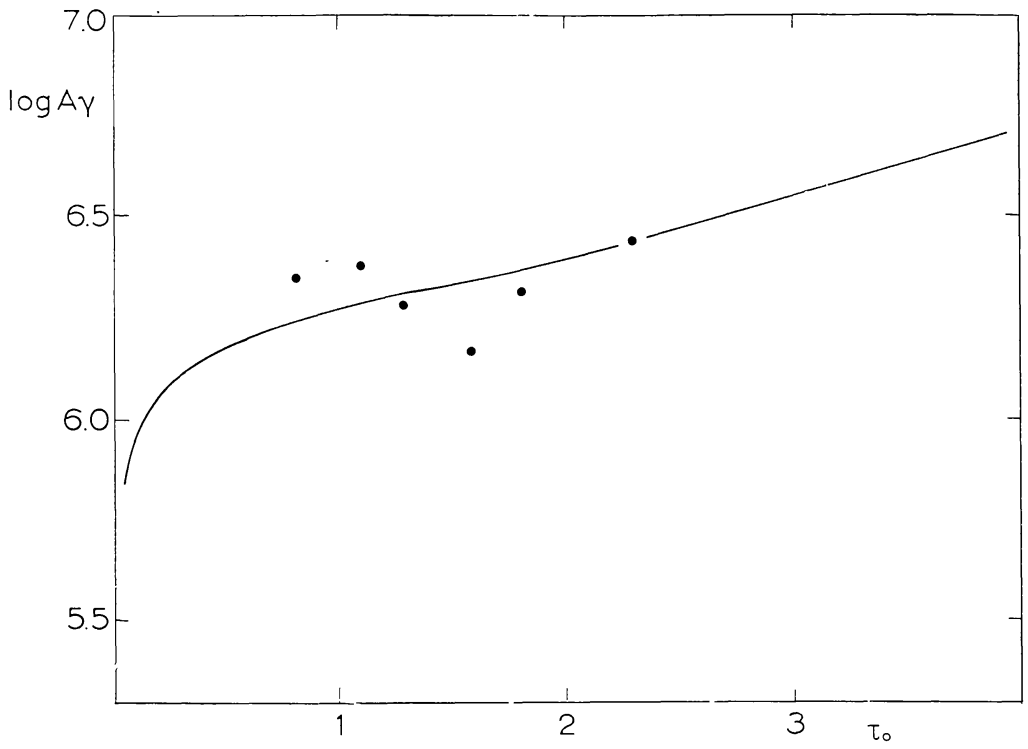

Fig. 4. Finally adopted $A_C\gamma(\tau_0)$ relation.

damping by the quadratic Stark effect of neighbouring electrons. It is possible to separate the two components from the observational results; hence, to find $\gamma_{H,He}(\tau_0)$ and $\gamma_e(\tau_0)$.

Theoretically, one knows that

$$\log \gamma_{H,He} = 3.84 + \log P_g + 0.7 \log \frac{5040}{T} + \\ + \log \left(\frac{n_0}{\sum n_r}\right)_H + \frac{2}{5} \log \left[\left(\frac{13.6\,Z}{\chi_r - \chi_{r,s}}\right)^2_{up} - \left(\frac{13.6\,Z}{\chi_r - \chi_{r,s}}\right)^2_{low}\right]$$

$\approx \log K_2 + \log P_g$, where K_2 is a very slowly varying function of depth.

For the electron broadening one has

$$\log \gamma_e = \log K + \log P_e + \frac{5}{6} \log \frac{5040}{T} \approx \log K_1 + \log P_e .$$

From the curve given in Figure 4, and using $\log A_C = 0.635 - 4$, one finds

$$K_1 = 5.40 \times 10^6 .$$
$$K_2 = 2.48 \times 10^4 .$$

The theoretical value for K_2 found from the above equation is 1.61×10^4.

The logarithmic difference between this theoretical value, and the experimentally determined one, is 0.2, which might indicate that the gas pressure $\log P_g$ has been assumed too small by about 0.2 in the region between $\tau_0 = 1$ and 2. So little is known of the gas pressure in the deep layers of the photosphere that such an increase of P_g should not be excluded *a priori*; however, we have to await the further analysis of other Fraunhofer lines before we shall be able to draw a final conclusion.

As to the electron broadening our result, $K_1 = 5.40 \times 10^6$ would give $\log K = 6.84$.

There are no measurements or theories yielding reliable values for K_1, but the value found here is of the same order as those derived from laboratory measurements for lines of similar elements. Altogether this is a reasonable agreement between the empirical solar values of $\gamma(\tau)$ and the values found from theory or expectation.

5. Determination of the Abundance A; Choice between two- and three-element Models

For a determination of the abundance of carbon the stronger lines of the multiplet are not suitable, because of two reasons:

(a) the cores of the strong lines are emitted by the uppermost parts of the photosphere, where the source function cannot be assumed equal to the blackbody function; neither are the *wing parts* suitable, since these are subject to the uncertainty of the γ-values;

(b) in the uppermost parts of the photosphere the microturbulent velocity component may be appreciable and may strongly influence the line profiles.

However, *the weaker lines* are emitted by the deeper photospheric levels, where microturbulence is weak. It is true that *convection* is appreciable in these layers but this quantity has been determined in section 3.

Furthermore the ambiguity still remaining between a two- and three-element model of the photosphere may be removed by considering the *widths* of relatively weak lines.

Our *procedure* is the following:

(1) We use the profile of the line λ 10754.02, observed in the centre of the disc; no centre-limb observations being available of this line. This line, which has a central residual intensity of 0.841 after correction for the apparatus profile, is reasonably weak, though not "weak" in the formal sense of the word, but this is not of importance.

(2) For this line we compute the central residual intensity for two variants of the U.R.P.-model, and for five arbitrarily chosen values of the product Afg.

Variant A: two-element model; U.R.P., with however $v_c = 0$ for $\tau_0 < 0.1$, and $v_c = 2.0$ km/sec for $\tau_0 > 0.1$.

Variant B: three-element model: U.R.P., with however $v_c = 0$ for $\tau_0 < 0.1$; $v_c = 3.1$ km/sec for $\tau_0 > 0.1$. The three elements of the photosphere are assumed to have the same area.

(3) A comparison of the computed and the observed central residual intensities yields by interpolation values of the abundance A_C for each of the two variants.

(4) Since the abundance A_C is then known, we also know γ, since in section 4 we

found $A_C\gamma$ as a function of the depth τ_0. We next compute for each of the two variants the whole line profile; a comparison of the results of the computations with the observations enables us to decide between the two variants.

Below we give some further details and results of the computations.

Step 1: The profile of the line, corrected for the influence of the apparatus is given in Table VI. For this line $\log gf = -1.58$ (GOLDBERG, MÜLLER and ALLER, 1960).

Steps 2 and 3: The central residual intensities were computed for the two variants, and for various values of the product $A_C\ gf$. From the results we derive as the "best" abundance: for the two-element variant (variant A): $\log A_C = 0.53 - 4$; for the three-element variant (variant B): $\log A_C = 0.63 - 4$.

TABLE VI

Observed and computed line profiles of the weak C I line at 10754 Å. The computations were made for $\log A = 0.635 - 4$. The zero point of the wavelength scale is not the same for the observed and the computed profiles (influence of convention)

		computed		
$\Delta\lambda$ (A)	obs	$S = B$	$S_1(\tau_0)$	$S_2(\tau_0)$
− .390	.983			
.360	.980			
.330	.977			
.300	.972	.982	.996	.988
.270	.966			
.240	.956	.954	.968	.959
.210	.946			
.180	.937	.916	.930	.920
.150	.914			
.120	.899	.879	.893	.881
.090	.869	.862	.878	.865
.060	.865	.848	.864	.852
.030	.846	.838	.856	.843
− .010		.836	.854	.842
0	.841	.836 5	.854	.843
+ .010		.838	.856	.844
.030	.848	.843	.861	.851
.060	.856	.857	.875	.865
.090	.874	.874	.892	.883
.120	.898	.894	.910	.902
.150	.925			
.180	.940	.932	.947	.940
.210	.948			
.240	.961	.966	.981	.974
.270	.974			
.300	.978	.989	1.003	.996
.330	.987			
.360	.991			
.390	.990			

Step 4: A detailed computation of the line profile was made next, for the two ariants, each of them with its "own" corresponding abundance. The computed alfwidths, as compared with the observed ones are:

for the two-element model	0.258 Å
for the three-element model	0.297 Å
observed	0.288 Å

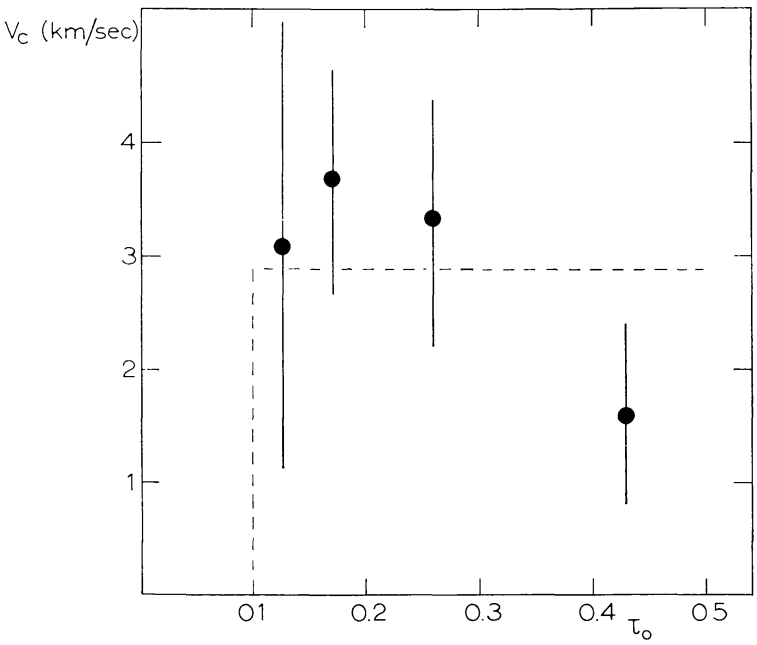

Fig. 5. Convective velocities v_c for a three-element photospheric model with a distribution of elements *hot* : *mean* : *cold* = $\frac{3}{8}$: $\frac{1}{4}$: $\frac{3}{8}$. The dashed line gives the adopted curve.

From this result we conclude that the three-element variant describes the observations better than the two-element variant does. If the small difference between the half-width computed for the three-element variant and the observed value is to be taken seriously one would conclude that the "best" subdivision of the photosphere should be:

Area of the hot and cold columns, each $\frac{3}{8}$,
Area of the average column $\frac{1}{4}$.
The abundance would then be: $\log A_c = 0.61 - 4$.

The corresponding convective velocity assumed constant with depth beyond $\tau_0 = 0.1$ would then be 2.9 km/sec.

We shall provisionally assume these latter results. In the next section the source function will be determined. It will then appear that the very center of the weak line is still slightly influenced by the fact that $S \neq B$ for $\tau_0 \lesssim 0.1$. This fact will force us to make a new determination of A_C after having found $S(\tau_0)$, and, after that, to determine a second approximation $S(\tau_0)$-curve (section 7). However, altogether it will appear that these second-approximation corrections to A_C and $S(\tau_0)$ are small.

6. The Source Function S(τ)

It is fairly certain that in the deep parts of the solar photosphere the source function $S(\tau)$ equals the *Planck* function; deviations from L.T.E. are only expected to occur in the high photospheric layers. For this reason it seems appropriate to use the *central intensities* of the stronger spectral lines of the multiplet for an empirical determination of the source function and its variation with depth in the photosphere. Another reason for using the central parts of the lines is that the absorption coefficient at the wavelength of the unshifted line centre can be computed fairly easily, though the treatment is complicated by the demand that the convective velocity and its variation with depth should be known. The convective velocities have been determined in section 3. In section 5 it was shown that the three-element variant represents the photospheric structure best.

A second complication in the treatment arises since the assumed abundance of carbon influences the results; it is not possible wholly to separate the effects of $S(\tau)$ and of A_C on the central line intensities. A first approximation value of A_C has been determined in section 5, by using the central intensity of a weak line. In that determination we assumed L.T.E. in the regions where this line is formed; it is shown in this section that this assumption is reasonable. A third complication may come from the influence of the microturbulent velocity field. The values of $\kappa(\Delta\lambda=0)$ are obviously influenced by the $v_t(\tau)$ curve. Hence, the derived $S(\tau)$ will depend on $v_t(\tau)$, but not very strongly so. The $v_t(\tau)$ relation will be determined in section 7. In view of this cross-relation between the deduced $v_t(\tau)$ and $S(\tau)$ curves, our procedure will be *first* to determine $S(\tau)$, using the A_C and v_c values found in sections 5 and 3, starting with a provisionally assumed $v_t(\tau)$ relation, namely that of the U.R.P. 1964 model.

With the resulting $S(\tau)$ function we shall compute the central intensities of the lines. Small differences with respect to the observed values will occur; this will lead to new A_C and S values, which are derived in section 7. In section 8 we shall compute $v_t(\tau_0)$.

If we call λ_0 the wavelength of the centre of the undisplaced line as it would occur in the solar spectrum if there was no convection, and $\Delta\lambda$ the wavelength distance between the center of the displaced absorption coefficient profile and λ_0, then

$$\Delta\lambda = -\frac{v_c}{c}\lambda,$$

where upward velocities are counted positive.

For each depth in the solar photosphere the selective absorption coefficient $\kappa(\lambda_0)$ (per gram of solar matter) at the wavelength λ_0 may be computed according to the expression

$$\kappa(\lambda_0) = \frac{\sqrt{\pi}\cdot e^2}{mc^2}\lambda_0^2\frac{b_{r,s}}{g}\,3.508\,10^{23}A_c g f\,\frac{\exp\left(-(\Delta\lambda/\Delta\lambda_D)^2\right)}{\Delta\lambda_D}, \qquad (18)$$

where

$$\Delta\lambda_D = \frac{\lambda}{c}\sqrt{\frac{2RT}{\mu} + v_t^2}$$

is the Doppler width.

An essential assumption underlying Equation (18) is that the central part of the line profile can be approximated by a Doppler profile. This approximation is acceptable since v_c and hence, $\Delta\lambda$ is small, so that the damping effect does not influence the value of $\kappa(\lambda_0)$. The total optical depth τ in the line center can easily be determined for a given model of the photosphere and the low chromosphere.

After that, the intensity in the line center can be computed. This has been done for the five strongest lines of the multiplet given in Table I, and for six values of $\cos\theta$, between 1.0 and 0.30. As a model we have used the Utrecht Reference Photosphere 1964 (URP). In order to obtain an empirical determination of the source function $S(\tau)$ we proceeded in four successive steps:

(1) Observed central residual intensity *times* absolute value of continuous intensity $\rightarrow$ observed intensity in the line center; that is $I(\cos\theta)$.

(2) $I(\cos\theta) \rightarrow S(\tau)$ via a Laplace transformation.

(3) The relation $\tau(\tau_0)$ is computed for the URP assuming the carbon abundance found in section 5.

(4) The deduced $S(\tau_0)$ is compared with the $B(\tau_0)$ function given by the model. For a consistent model one must have $S(\tau_0)=B(\tau_0)$ for the weakest line, since the discussion of section 5 was based on that assumption.

Step 1: The continuous intensity at 10700 Å, computed for the U.R.P. model and for various values of $\cos\theta$, was multiplied by the observed residual intensities in the five lines (functions of $\cos\theta$) to give the "observed" absolute intensities in the line centers (see our remark on pag. 32).

Step 2: By a least-squares procedure $I(\cos\theta)$ was represented by a second degree polynomial

$$I(\cos\theta) = a + b\cos\theta + c\cos^2\theta\,.$$

Then it follows that

$$S(\tau) = a + b\tau + \frac{c}{2}\tau^2\,.$$

Here τ is the monochromatic *total* optical depth in the line center (sum of continuous and selective optical depths).

Step 3: Since there is no empirical way of determining the relation between τ and τ_0, where τ_0 is the monochromatic optical depth in the continuous spectrum at 5000 Å, we must compute this relation. This was done, assuming L.T.E., the URP model, and the carbon abundance found in section 5 ($\log A_C = 0.61-4$). Once such a relation has been derived, we can transform $S(\tau)$ into $S(\tau_0)$. This result can then be compared with $B(\tau_0)$ for the model, where B is the Planck function. If it turns out that $S = B$, our three assumptions could be correct; if not, one or more of them may be in error, either the model, or the abundance, or the assumption of L.T.E.

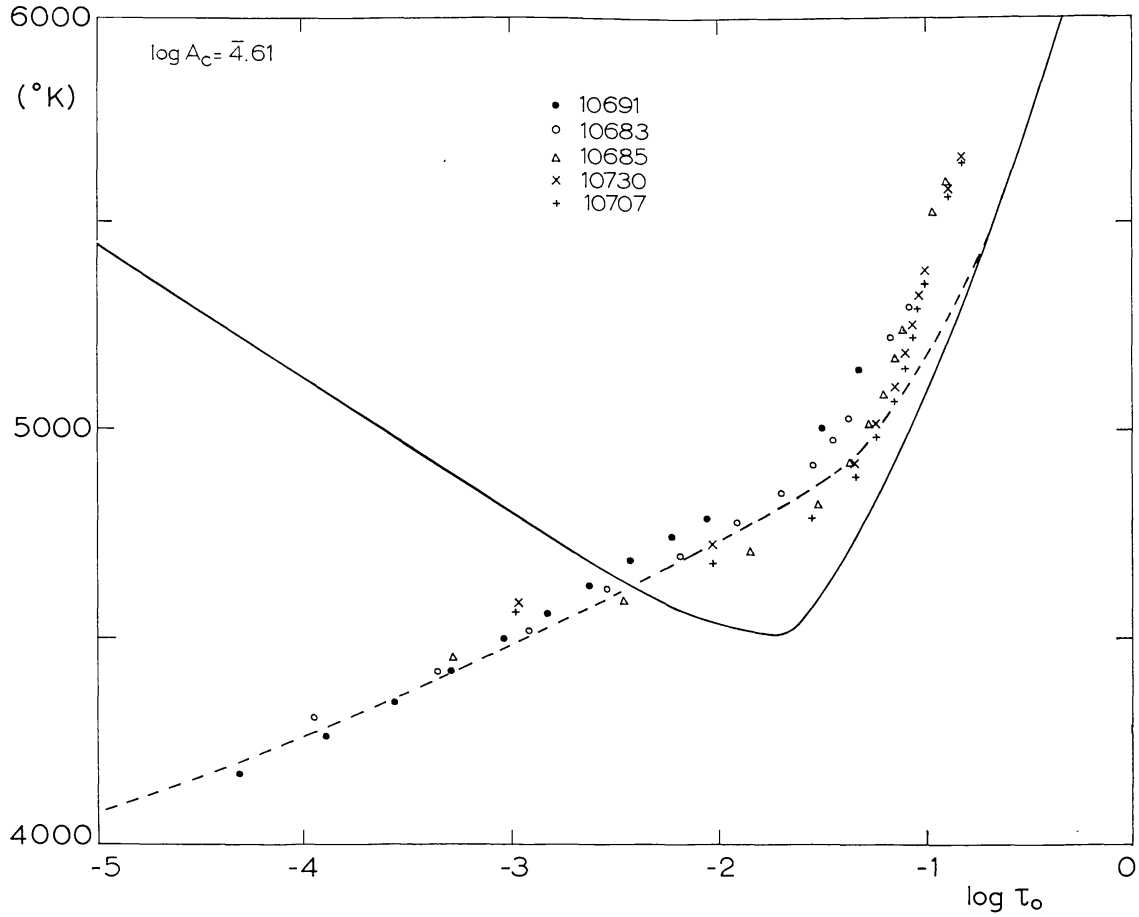

Fig. 6. Empirically determined source function $S(\tau_0)$ for the lines of the C I multiplet for $\log A_C = 0.61 - 4$.

The relation between τ and τ_0 was computed for the U.R.P. model, but only for *the average component* of it. This simplification is correct only for the parts of the lines that are formed in layers for which $\tau_0 < 0.1$. In deeper layers convection will play a part. It will turn out that this simplification is not fully justified for the three weakest lines, so that a correction has to be applied to the results derived from these lines.

The resulting $S(\tau_0)$-values, expressed through Planck's law in excitation temperatures, are shown in Figure 6. The solid line gives the kinetic temperatures (corresponding to $S = B$); the various symbols give T_{ex} for the cores of the five strongest lines, and for various τ_0-values.

The *main result* is that the assumption of deviations from L.T.E. is inevitable for $\tau_0 < 0.1$. In fact $S(\tau_0)$ *de*creases continuously outward, whereas $B(\tau_0)$ *in*creases outward for $\tau_0 < 0.02$. In view of the strong evidence from many sources for an increase of T in the low chromospheric layers it seems impossible to change the model in such a way that S would become equal to B. Consequently Kirchhoff's law does not represent line formation at $\tau_0 < 0.1$.

There is another result that needs some attention. At $\tau_0 \approx 0.07$ there seems to occur a fairly sharp kink in the $S(\tau_0)$-curve; for larger τ_0-values ($\log \tau_0 > -1.2$), $S(\tau_0)$

seems to run almost parallel to the $B(\tau_0)$-curve. Contrary to what would be expected it looks as if $\lim_{\tau\to\infty} S(\tau) \neq B(\tau)$.

This phenomenon can be explained fairly easily. It is due to the influence of convection which, as we know from section 3, starts rather abruptly near or even slightly below $\tau_0 = 0.1$; v_c reaches fairly high values already at that level. The fact that the τ_0-values corresponding to certain specific S-values had been computed for the average photospheric model, neglecting convection, made our absorption coefficients too large, and the resulting τ_0-values too small.

Hence we have got here another, *independent* indication that convection starts close to $\tau_0 = 0.1$.

It is possible to estimate the convective velocities, necessary to bring $S(\tau_0)$ in agreement with $B(\tau_0)$ for $\tau_0 \approx 0.1$. The average horizontal distance between the $S(\log \tau_0)$ and $B(\log \tau_0)$ curves is: $\Delta \log \tau_0 \approx 0.3$, so that the average absorption coefficients used in the computation were too large by a factor 2 approximately. Hence, if $\Delta\lambda$ is the displacement of the lines due to convection, then the average reduction in κ due to convection is:

$$\tfrac{1}{4} + 2 \times \tfrac{3}{8}(\exp(-/\Delta\lambda/\Delta\lambda_D)^2) = 0.5\,.$$

Hence, with $T \approx 5500°$ and $v_t \approx 1.5$ km/sec, one would obtain $v_c = c\Delta\lambda/\lambda = 3.3$ km/sec. This value turns out to be closely equal to the average convective velocity derived in sections 3 and 5 (there we found $v_c \approx 2.9$ km/sec).

This result shows again that the convective velocities reach values of about 3.0 km/sec near $\tau_0 = 0.1$ (again supporting the *three-column* model), and the position of the kink in the $S(\tau_0)$ curve suggests that convection starts rather sharply near $\tau_0 = 0.08$.

Also this result is in agreement with the finding in section 3.

We are now in a position to draw an average $S(\tau_0)$ curve, which is the broken line in Figure 6. The extrapolation between $\log \tau_0 = -1.2$ and -0.8 is not certain but can never be very much in error. We should further stress that this part of the photosphere is the most difficult part for the present discussion since at least three effects combine in this region and cannot be separated, namely deviations from L.T.E. and the influence of v_c and v_t.

For $\log \tau_0 < -4.5$ the source function is not known but we have smoothly extrapolated the empirical $S(\tau_0)$ curve down to an excitation temperature of 3800° which seems to be the limiting photospheric excitation temperature, as may be inferred from the central intensities of very strong fraunhofer lines.

Verification of result: With the $S(\tau_0)$ curve thus obtained we computed the profile of the weakest line (λ 10754) for the centre of the disc. The computations were made with the parameters (T, P_e, P_g, v_c, v_t) of the U.R.P.-model, assuming *three* columns, with the weighting factors as determined in section 5, the $S(\tau_0)$ curve derived above, and $\log A_C = 0.61 - 4$.

For this line we found:

computed central residual intensity	0.848,
observed value	0.841.

The fact that these values are not equal indicates the influence of the $S(\tau_0)$ curve being unequal to $B(\tau_0)$ at $\tau_0 < 0.1$. With the given abundance assuming $S(\tau_0) \equiv B(\tau_0)$, we should have found the observed value. This compels us to apply a small correction to the A_C-value derived in section 5.

7. Second Approximation Values of A_C and of $S(\tau_0)$

With the $S(\tau_0)$ curve of Figure 6 a new relation was computed between I/I_0 and log *Agf*. This relation appears to be nearly linear in the range of interest. In order to equalize the observed and computed values of the residual central intensities it appears necessary to change A_C slightly and to take

$$\text{Log } A_C = 0.635 - 4.$$

However, the assumption of another A_C-value also changes $S(\tau_0)$. With this new value for the abundance the procedure from section 6 for determining $S(\tau_0)$ was repeated; the resulting new $S(\tau_0)$ points are given in Figure 7. Table VII compares our final value of the abundance with other values.

It is obvious, from comparison of Figures 6 and 7, that there is no great difference

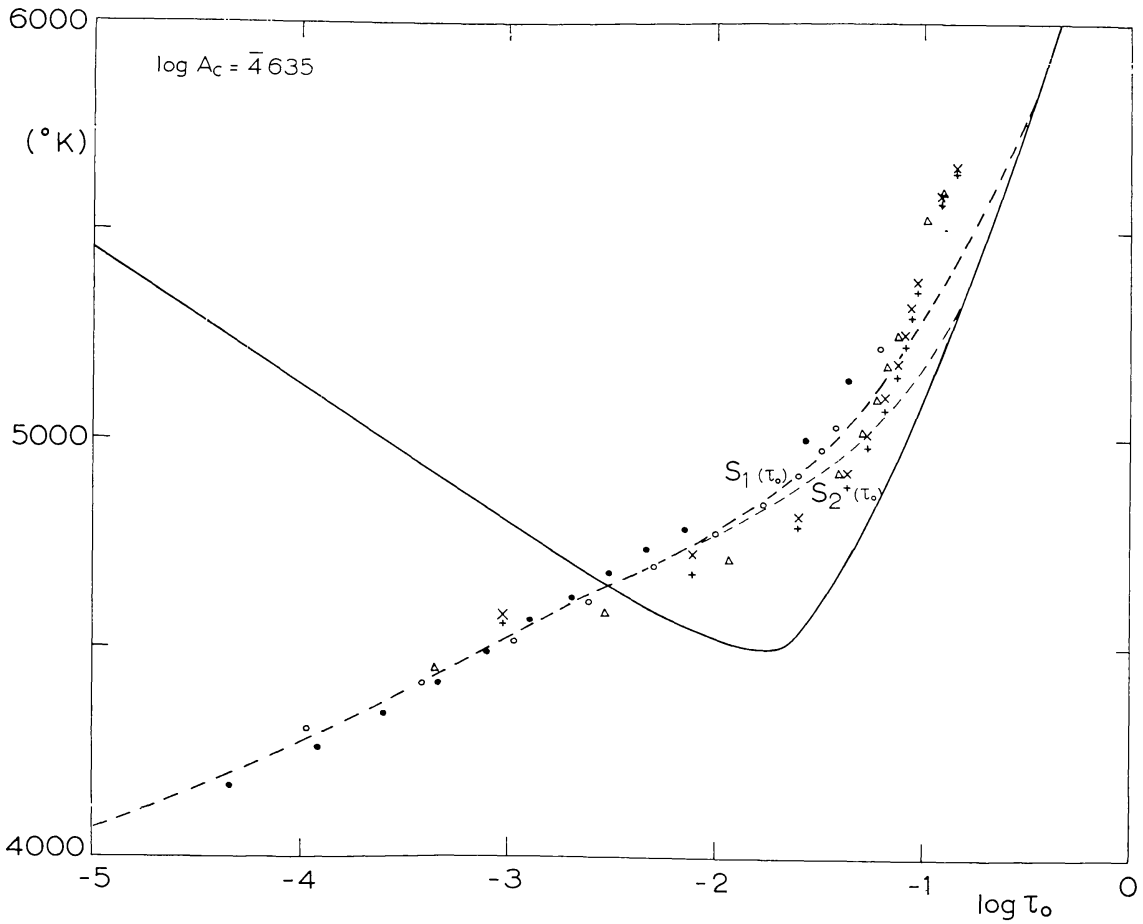

Fig. 7. Empirically determined source function $S(\tau_0)$ for the C I multiplet for log $A = 0.635 - 4$.

TABLE VII

Some recent determinations of the solar abundance of carbon

Author	$\log A_C + 12$
GOLDBERG, MÜLLER, and ALLER (1960)	8.72
BASCHEK (1962)	8.65
ANDREWS and MUGGLESTONE (1963)	8.68 (Aller-Pierce model) 8.69 (Swihart model) 8.77 (De Jager model)
SCHADEE (1964) (from molecules)	8.55 ± 0.17
This paper	8.635

between the two $S(\tau_0)$ curves. It is, furthermore, important to notice that there is a certain scattering in the points due to the uncertainties in the observations.

In order to show the limitations caused by these uncertainties we have drawn *two* possible T_{ex}-curves representing $S(\tau_0)$. Henceforth we shall call the corresponding source functions $S_1(\tau_0)$ (the uppermost curve) and $S_2(\tau_0)$. We think that $S_2(\tau_0)$ may be a better representation than $S_1(\tau_0)$.

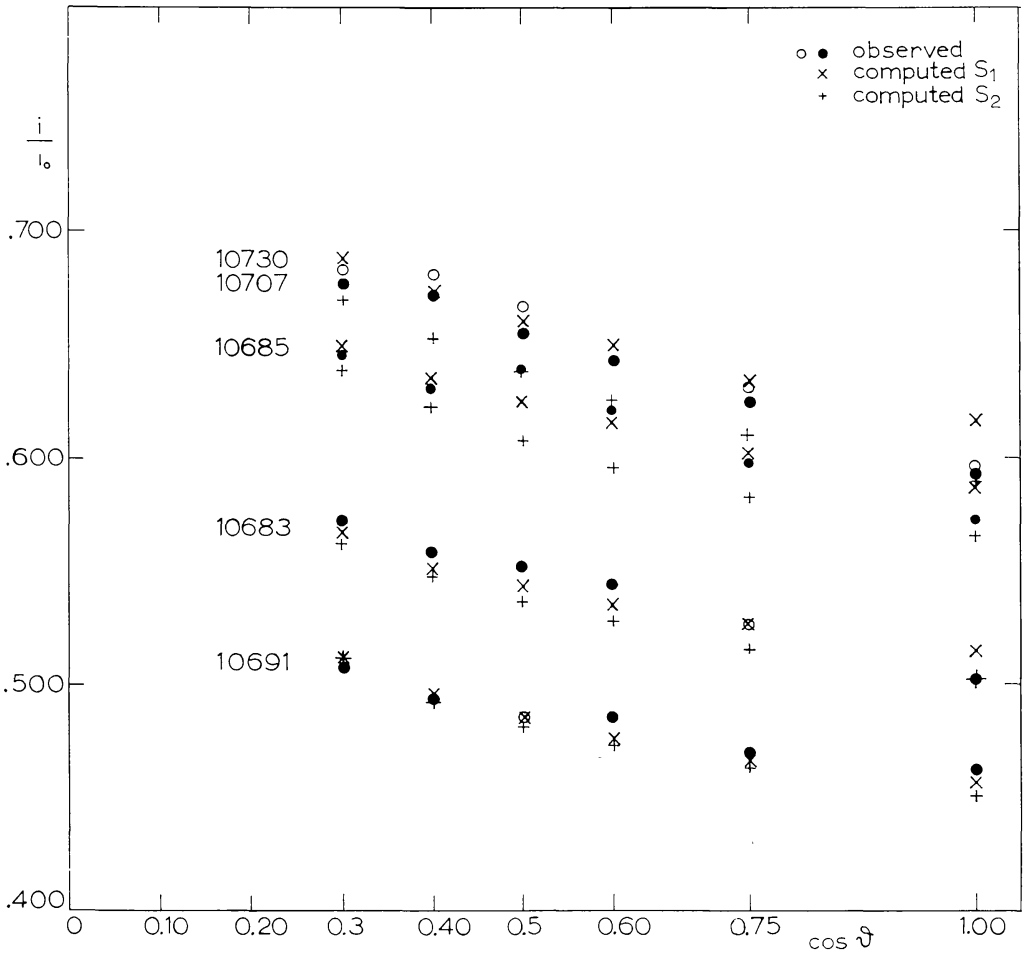

Fig. 8. Comparison of observed and computed central intensities for the five strongest lines of the multiplet assuming the $S_1(\tau_0)$, and the $S_2(\tau_0)$ curves.

With the two adopted $S(\tau_0)$ curves we have computed the central intensities for the five strongest lines for all six values of cos θ. These results are shown in Figure 8.

Furthermore we give in Figure 9 the computed and observed profile of the weak line at 10754 Å for the L.T.E. case and for the two $S(\tau_0)$ curves.

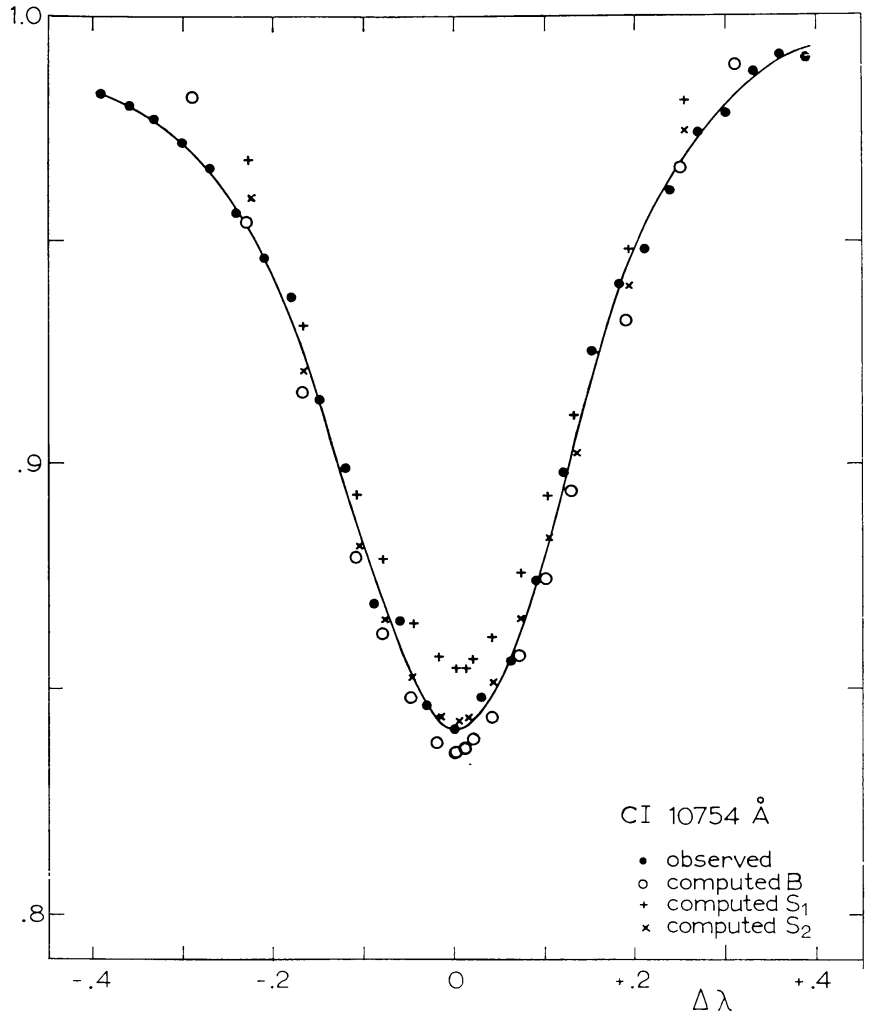

Fig. 9. Observed and computed line profiles of the weak line at 10754 Å. The computations were made for the L.T.E. case (S ≡ B), and for the two $S(\tau_0)$ curves of Figure 7, and assuming $\log A_C = 0.635 - 4$.

Figures 10 to 14 inclusive give the complete observed line profile of the stronger lines for the six values of cos θ, compared with the computed profiles. The computations were made for the line center and the wings; they have not yet been made for the central parts of the profiles; these parts can only be computed after a determination of the turbulent velocity component $v_t(\tau_0)$. On the other hand, the influence of turbulence is not very important for the weak line (Figure 9), since this line is formed in fairly deep layers, where turbulence is unimportant.

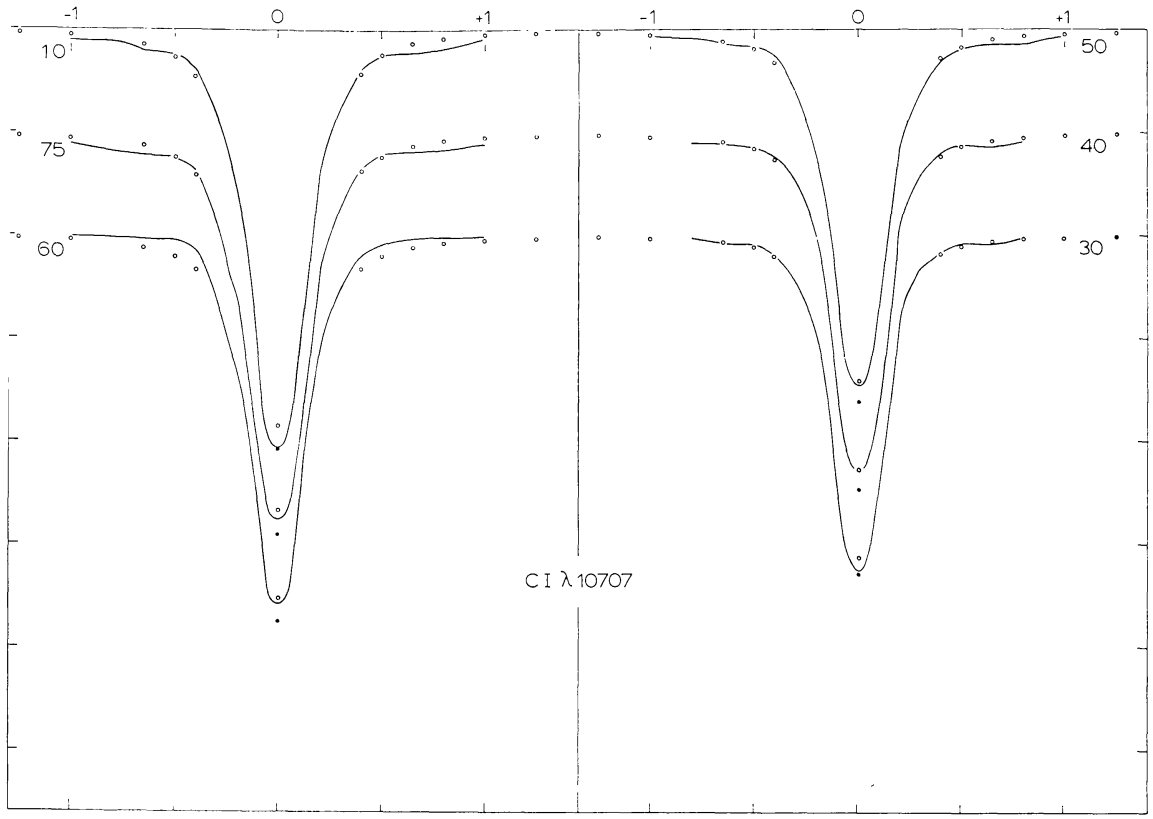

ig. 10. Observed and computed line profiles for λ 10707; open circles: computed with B or S_1; filled circles: computed with S_2. The line gives the observed profile.

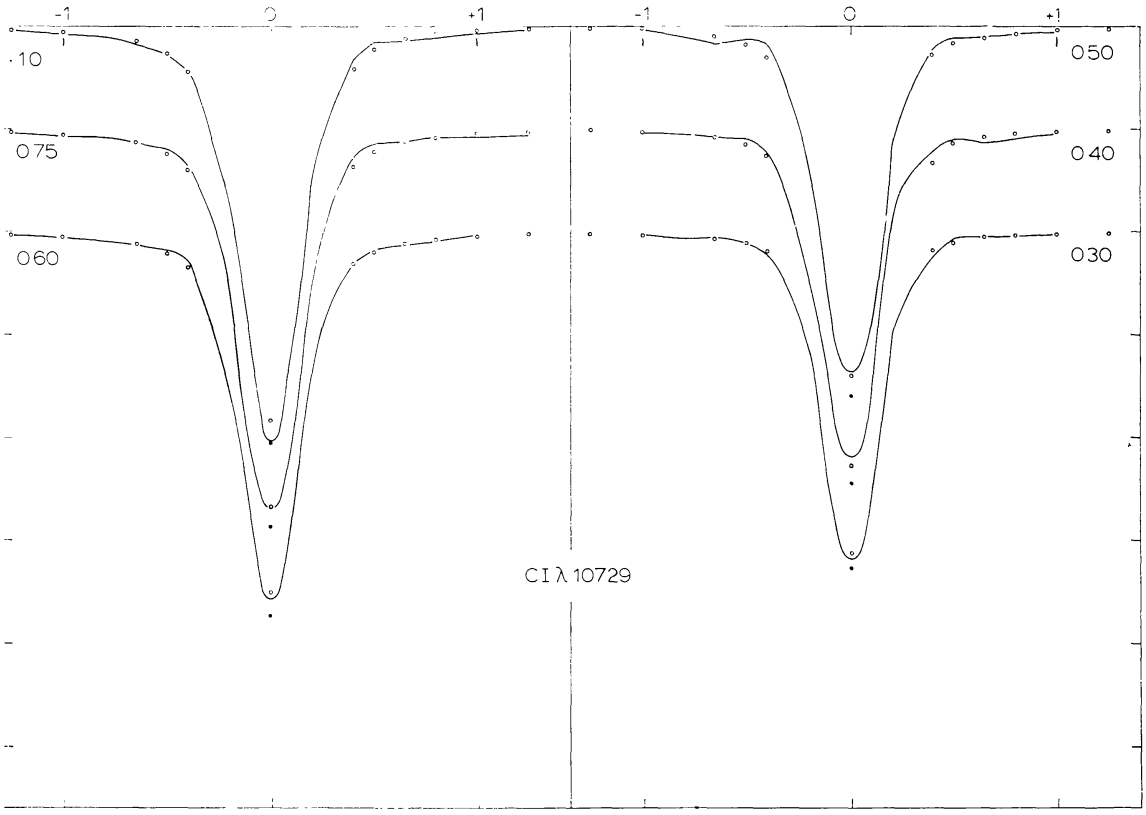

Fig. 11. Line profiles of λ 10730.

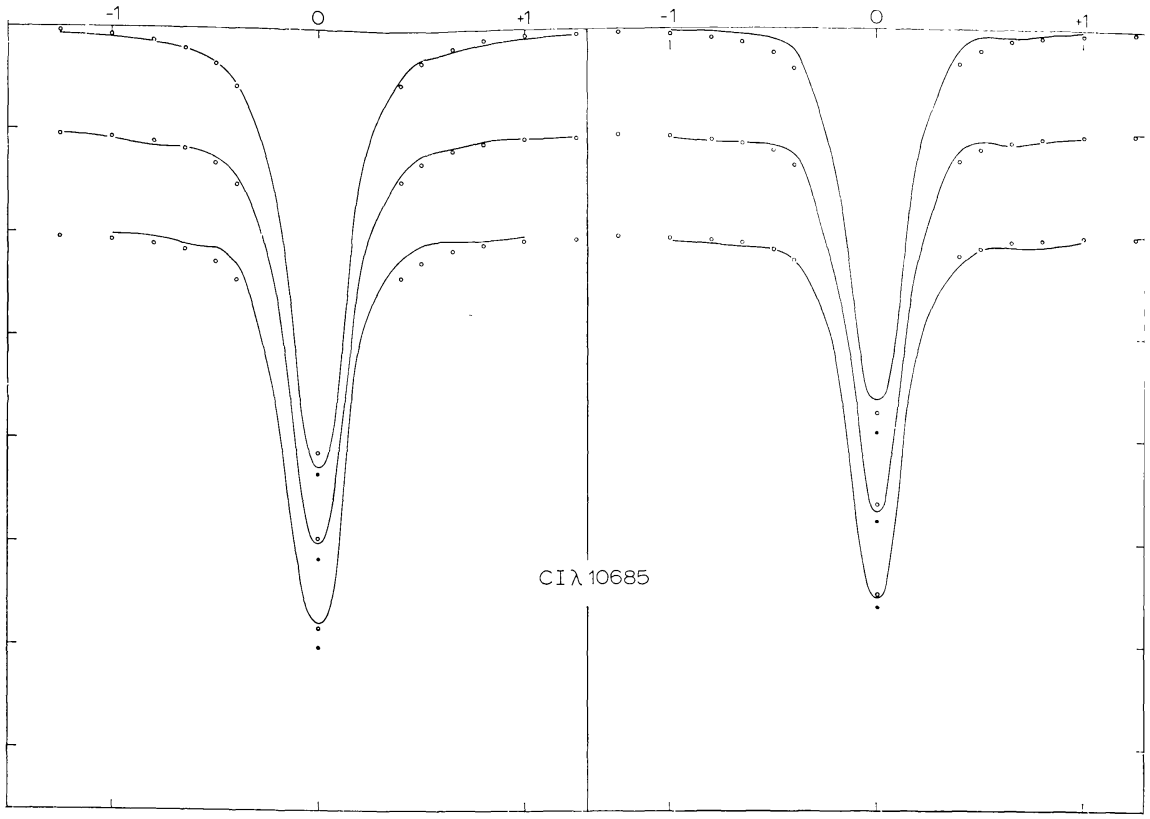

Fig. 12. Line profiles of λ 10685.

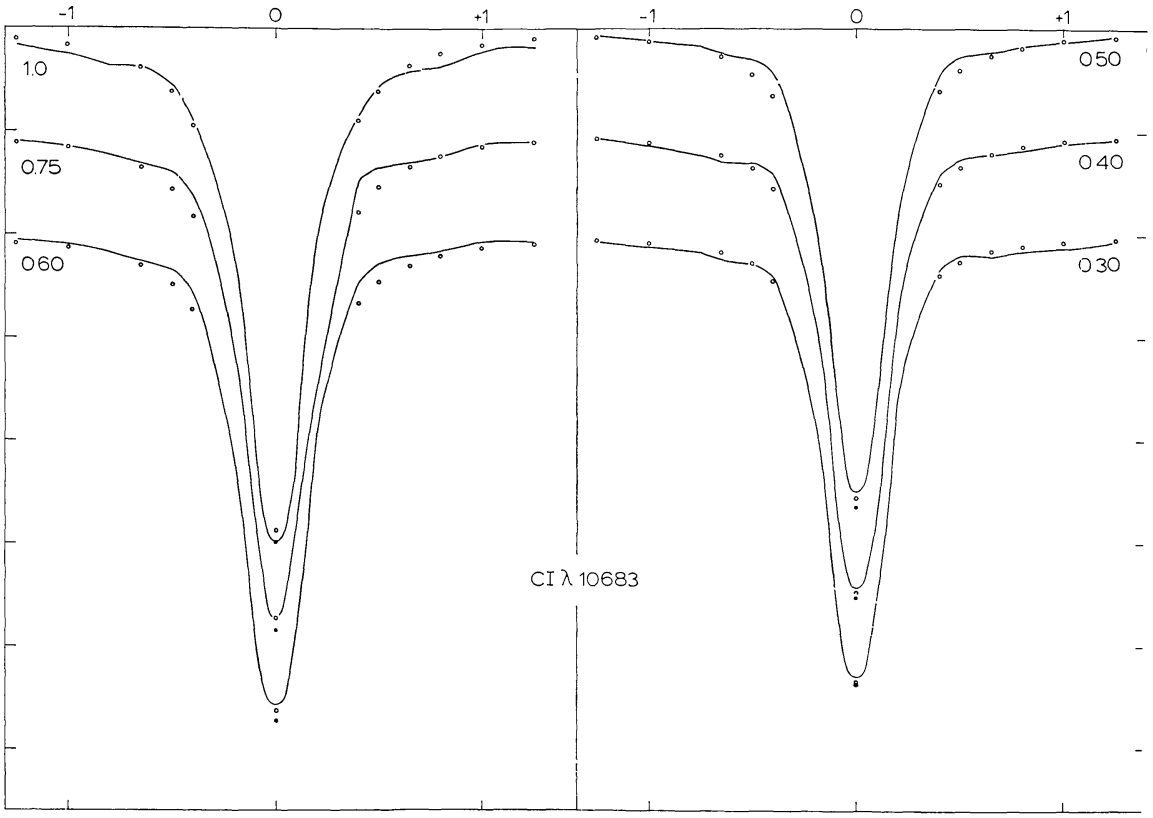

Fig. 13. Line profiles of λ 10683.

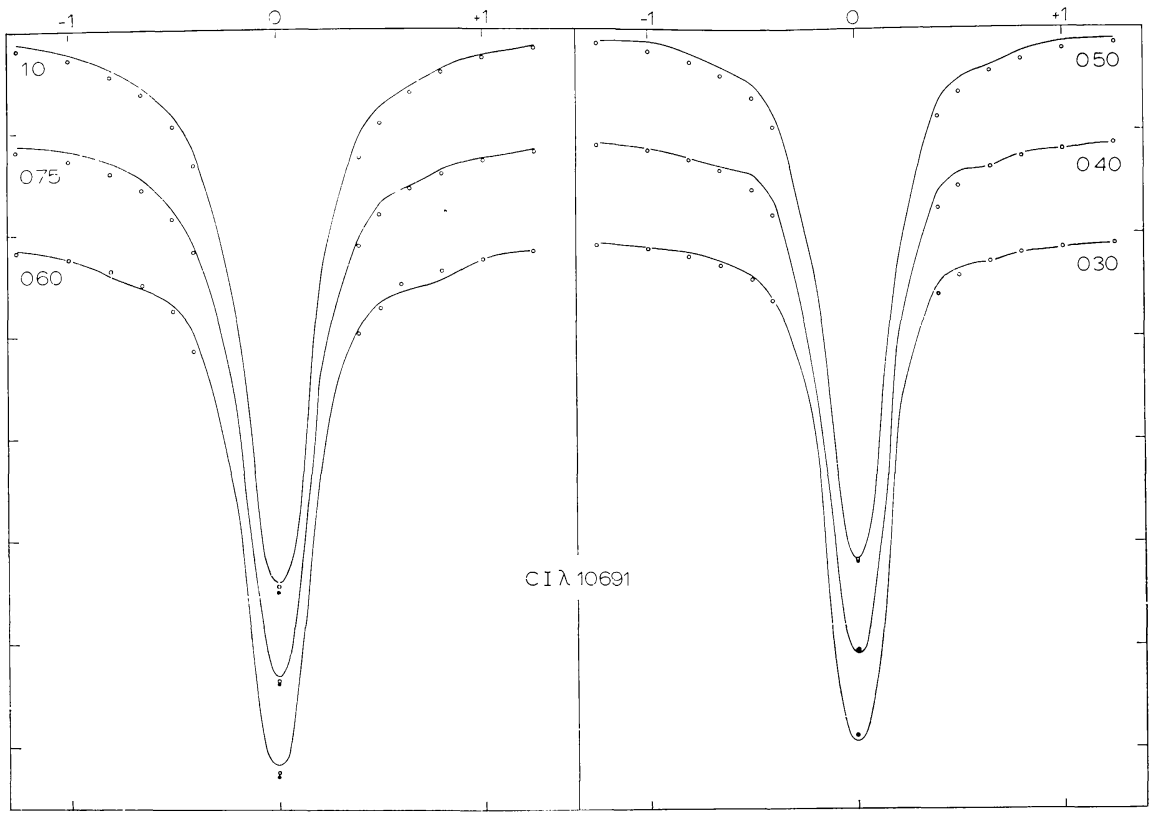

Fig. 14. Line profiles of λ 10691.

A summary of the main results shown in Figures 8 to 14 may be formulated as follows:

If we assume

log $A_C = 0.635 - 4$;

the $S_2(\tau_0)$ curve of Figure 7;

$v_c = 2.9$ km/sec for $\tau_0 \geqslant 0.1$;

the γ-values from Figure 4;

$\varphi(v_c)$ according to the subdivision hot : average : cool elements $= \frac{3}{8} : \frac{1}{4} : \frac{3}{8}$;

the v_t curve for the U.R.P. 1964,

then one obtains a good agreement between observations and computations for the three strong lines of the multiplet. For the weaker lines the computed central intensities are a bit too low, but the deviations from the observed values are completely within the range of uncertainty of the $S(\tau_0)$ curve, as may be inferred from a comparison of the results computed for $S_1(\tau_0)$ and for $S_2(\tau_0)$.

Hence there is no use in attempting to find further approximations to A_C and/or $S(\tau_0)$. The accidental probable error in log A_C may be estimated at $\pm$ 0.01 or 0.02, apart from a possible uncertainty in the assumed log *gf*-value which may be the source of larger *systematic* errors. We may further point out that the main source of error in solar abundances is now the *gf*-values, uncertainties in the photospheric model do not play a part. See also Table VII.

8. The Microturbulent Velocity Component and its Variation with Depth

The line of sight microturbulent velocity component has been determined from the line profiles by the method of Goldberg-Unno:

For two lines with *gf*-values $(gf)_1$ and $(gf)_2$ we measure the line widths $2\Delta\lambda_1$ and $2\Delta\lambda_2$ at the same value of the depression d. We take care of measuring $2\Delta\lambda_1$ and $2\Delta\lambda_2$ in the deepest central part of the line, where the profile of the absorption coefficient may still be assumed to be symmetric and to have a Gaussian shape, and where the influence of convection may be neglected.

Since the lines occur in the same wavelength region and are due to the same element and are part of the same multiplet, the selective absorption coefficients necessary to produce a depression d in the two lines must be equal. Hence

$$(gf)_1 \exp\{-(\Delta\lambda_1/\Delta\lambda_D)^2\} = (gf)_2 \exp\{-(\Delta\lambda_2/\Delta\lambda_D)^2\}$$

With the given *gf*-ratio and the measured $\Delta\lambda$ values we may solve for $\Delta\lambda_D$ from any pair of lines and for any depression d. This was done for d-values of 0.05; 0.10; 0.15 ... etc. It then appeared that all results derived from the largest d-values (smallest $\Delta\lambda$-values) yielded the same $\Delta\lambda_D$-values, at least for a given value of $\cos\theta$, but that measurements taken at smaller depressions yielded larger values of $\Delta\lambda_D$. This is to be expected. At small d-values the absorption coefficient profile is no longer Gaussian, and damping and the additional broadening by convective motions play a part.

For each value of $\cos\theta$ a histogram of all the derived values of $\Delta\lambda_D$ was made for all possible combinations of the lines. One then obtains a definite clustering of the values of $\Delta\lambda_D$ near a small value (see Figure 15). Larger values occur also, but these are far more scattered and are clearly the result of measurements at values of the depression too small to have only the influence of turbulence. The extra broadening for smaller values of d is due to the fact that for these values convection plays a part in broadening the line profile. The role of convection as a broadening mechanism, and the consequent errors creeping into the results derived by the Goldberg-Unno method, have never been well estimated or described. Part of the strange results derived by this or similar methods within the last few years may be ascribed to this neglect.

The center of gravity of the maximum in the $\Delta\lambda_D$-histogram for small values was taken as the "best" $\Delta\lambda_D$-value. We thus got the results presented in Table VIII (second column). The average line depression d to which these measurements apply has been derived and is given in Table VIII, third column.

Clearly these results have to be transformed into a curve that gives the variation of the average particle velocity, or better: of the microturbulent velocity component with depth, or with $\cos\theta$, in the atmosphere. Such a derivation was made, based on the assumption that an emergent intensity I is mainly emitted by the layers where $\tau_{\text{total}} \approx 1$, so that the source function $S(\tau = 1) = I$. With this assumption, and using the $S_2(\tau_0)$ curve derived in the preceding section an observed intensity I immediately gives $S\ (= I)$, and hence T_{ex}, T_{kin} and the average optical depth of emission which

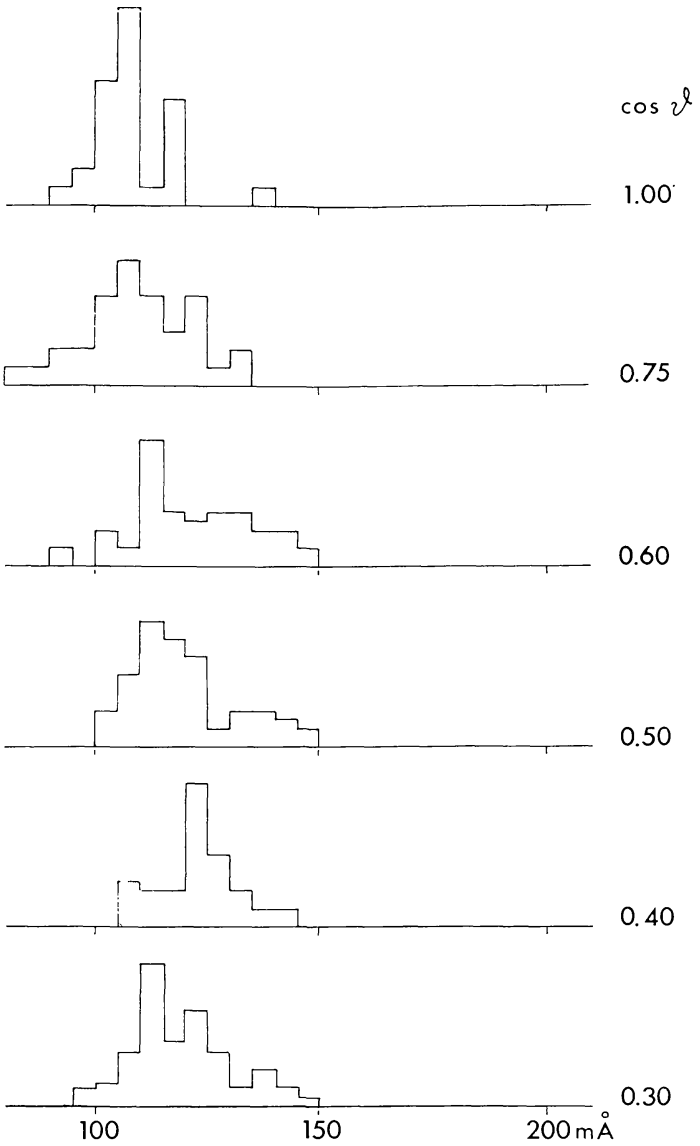

Fig. 15. Statistics of the derived values of $\Delta\lambda_D$.

we shall call τ_0^*. A short computation then yields the v_t-values given in Table VIII. It is seen from this table that the first v_t-value is certainly not fully reliable since τ_0^* appears to be too large and to lie in the region where convection is not negligible,

TABLE VIII

Doppler widths of C I lines, and microturbulent velocities

cos θ	$\Delta\lambda_D$	$\bar{d}$	T_{kin}	τ_0*	v_t (km/sec)
1.00	0.1085	0.32	5190	0.12	1.44
0.75	0.109	0.30	5015	0.085	1.55
0.60	0.118	0.30	4835	0.058	2.06
0.50	0.116	0.27	4820	0.055	1.98
0.40	0.1235	0.27	4630	0.034	2.36
0.30	0.115	0.20	4730	0.044	1.97

so that *this* v_t-value must be an upper limit (indicated by the symbol $\vee$ in Figure 16).

In Figure 16 these velocity components are plotted against "their" τ_0^*-value, and compared with the $v_t(\tau)$ values of the U.R.P. model. The agreement seems reasonably satisfactory and may be reconciled with theoretical ideas, according to which the "microturbulence" should in reality be interpreted as a field of pressure waves emerging from the convection zone and propagating outward. If there was no dissi-

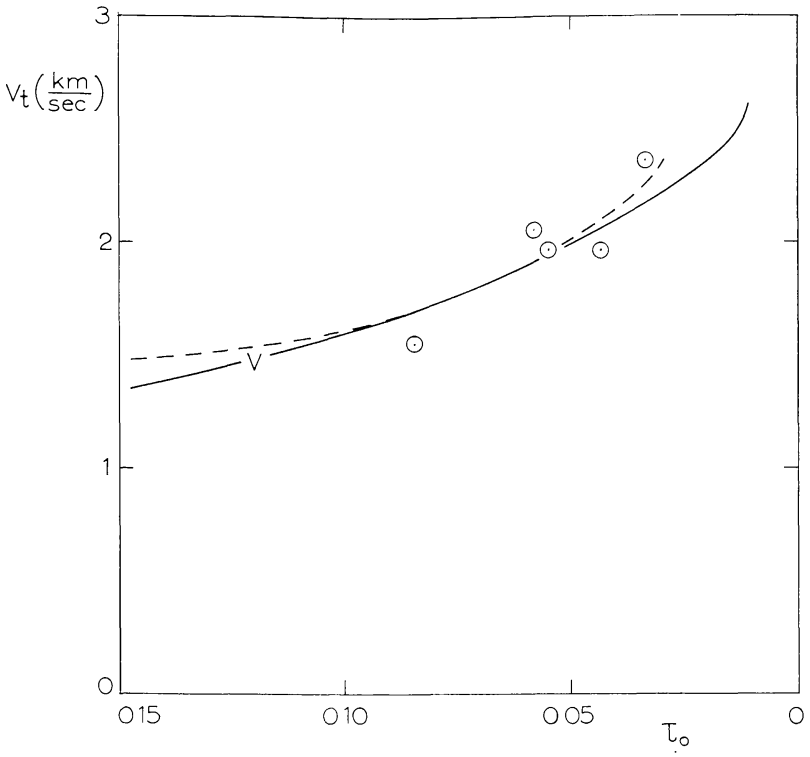

Fig. 16. Turbulent velocities in the upper photosphere computed with the $S_2(\tau_0)$ curve of Figure 7. The solid line gives the relation assumed in the U.R.P. model. The dashed line corresponds to the relation $v_t = \text{const.}\, P^{-\frac{1}{2}}$. The value of the constant has been adapted.

pation of energy the $v_t(\tau)$-variation would be steepest. In that case, since the flux of pressure waves

$$F_p = \tfrac{1}{2}\rho v_t^2 v_{\text{sound}} = \text{constant},$$

and since $v_{\text{sound}} \approx$ constant:

$$v_t(:)\rho^{-\frac{1}{2}}(:)P^{-\frac{1}{2}}.$$

This latter relation is represented by the dashed curve in Figure 16, which agrees fairly well with the observed v_t-values and with the solid line ($= v_t$-values from the U.R.P.-model). This suggests that dissipation of mechanical energy is not very important in those parts of the photosphere for which $\tau_0 > 0.04$.

Since our empirical v_t-values agree with the U.R.P. v_t-values, on the basis of which the $S(\tau_0)$ curve was determined in section 6 it is apparently not necessary to determine $S(\tau_0)$ anew in a third iteration by using the new v_t-values. In fact, because of the

smallness of the differences between the empirical v_t-values found here, and these assumed for the U.R.P. 1964 model we tend to consider the new results as a confirmation of the v_t-values assumed in the U.R.P. 1964 model.

Acknowledgment

All the numerical work and the programming involved in the computations presented here, have been made by Mr. W. Nijs (Uccle Observatory). Without his energetic assistance this work would not have been finished. We thank him most cordially for the efficient way he contributed to this investigation. We are also thankful to Prof. Anne B. Underhill (Utrecht) for a number of editorial remarks.

References

ANDREWS, M. and MUGGLESTONE, D.: 1963, *Mon. Not. R. Astron. Soc.* **125**, 347.
BASCHEK, B.: 1962, *Zeitschr. für Astrophys.* **56**, 207.
DE JAGER, C. and NEVEN, L.: 1964, *Mém. Soc. Roy. Sci. Liège* (5), **9**, 213 (= Liège Colloquium 1963).
DE JAGER, C. and NEVEN, L.: 1966a, I.A.U. symposium no. **26**: *The Abundance Determination in Stellar Spectra*, 149.
DE JAGER, C. and NEVEN, L.: 1966b, *J. Quantitative Spectroscopy and Radiative Transfer* **6**, 93.
DE JAGER, C. and NEVEN, L.: 1967, *Bull. Astron. Inst. Netherlands, Suppl. Series* (in press).
HEINTZE, J. R. W., HUBENET, H., and DE JAGER, C.: 1964, *Bull. Astron. Inst. Netherlands* **17**, 442.
GOLDBERG, L., MÜLLER, E. A., and ALLER, L. H.: 1960, *Astrophys. J., Suppl. Series* **45**, 1.
SCHADEE, A.: 1964, *Bull. Astron. Inst. Neth.* **17**, 311.